Crossrail Farringdon Eastern Ticket Hall (XTE12)

Report on human remains from Charterhouse Square Grout Shaft, London EC1

D Walker

MOLA

46 Eagle Wharf Road

London

N1 7ED

020 7410 2200

04/12/2013

HUM/REP/10/13

1 Introduction

This report presents the results of the analysis of human skeletal remains recovered during work to construct a 4m diameter circular grout shaft in the south-west corner of Charterhouse Square, London EC1, between February and March 2013 (site code XTE12). These works formed part of the archaeological investigations for the Crossrail Farringdon Eastern Ticket Hall development (Pfizenmaier 2013). The works revealed part of a medieval burial ground consisting of at least two north-south rows of extended and supine articulated inhumations, representing 25 individuals. Disarticulated human bone from a minimum number (MNI) of four individuals was also recovered.

The articulated remains were buried in three clear phases of activity. The earliest of these contained 11 inhumations, the second just two, and the third 12. Phase 1 and phase 2 burials were aligned south-west to north-east (head to foot). The third phase revealed a slight but distinct shift in burial alignment: west to east (head to foot), perhaps reflecting a period of a hiatus in funerary activity. In some cases, phase 2 burials were disturbed by the digging of phase 3 graves, with some bone re-deposited in the grave of the new burial. This supports the possibility of a hiatus, as does the level of decomposition suggested by the absence of articulation in the disturbed remains, which would not be consistent with the recently dead. The radiocarbon dating of tooth root collagen placed the first two phases of burial in the 14th century and the third phase in the first half of the 15th century.

The burials were found in an area believed to have been known as Spitalcroft in the 14th century. This land was leased by Sir Walter Manny from St Bartholomew's Hospital specifically for use as an emergency cemetery for the Black Death and was opened in late 1348 or early 1349. This extended the area available for burial following the opening of a similar ground at Pardon Churchyard, also known as 'Nomanneslond', to the north of Charterhouse. Together these grounds became known as West Smithfield (Barber and Thomas 2002, 12). The Carthusian Charterhouse was established on the site to the north of the square in 1370 (ibid 16–17).

Following excavation, a coordinated programme of pathogen DNA sequencing, stable isotope analysis and radiocarbon dating was carried out on 12 dental samples and one bone sample from the skeletal assemblage.

The human bone assessment identified potential areas of interest, in particular the possibility that at least some of the burial sample were exposed to or suffering from plague when they died (Walker 2013, 14). Recent developments in aDNA sequencing techniques, together with work on the East Smithfield emergency Black Death burial ground (Bos et al 2011; Schuenemann et al 2011), suggested it might be possible to identify the *Yersinia pestis* pathogen in the tooth samples. Such information, if obtainable, would contribute to our knowledge of the epidemiology and evolution of plague, and its interaction with human populations and environments over time. Of the 12 individuals sampled, four were confirmed to have been exposed to *Yersinia pestis*. These four burials spanned all three phases of burial.

This report contains details of the stable isotope analysis carried out on 10 tooth samples, providing information on the diet, levels of stress, and origins of the individuals within the burial sample (Montgomery et al 2014) (4.4).

This report also includes details of human bone recovered during a targeted watching brief at 23–28 Charterhouse Square and from utility diversions at the south-western corner of the square (XFS10) (MOLA for Crossrail 2012a, 2012b).

2 Nature of the sample

A minimum of 25 articulated individuals and four disarticulated individuals were excavated at XTE12, representing a total MNI of 29.

A minimum of two individuals were recovered from 23–28 Charterhouse Square and three individuals from utility diversions at the south-western corner of the square (XFS10) Further details of XFS10 are listed in the appendix 7.1.2.

2.1 Preservation

The majority of the articulated sample was well preserved (18/25: 72%) (Fig 1). No contexts were poorly preserved.

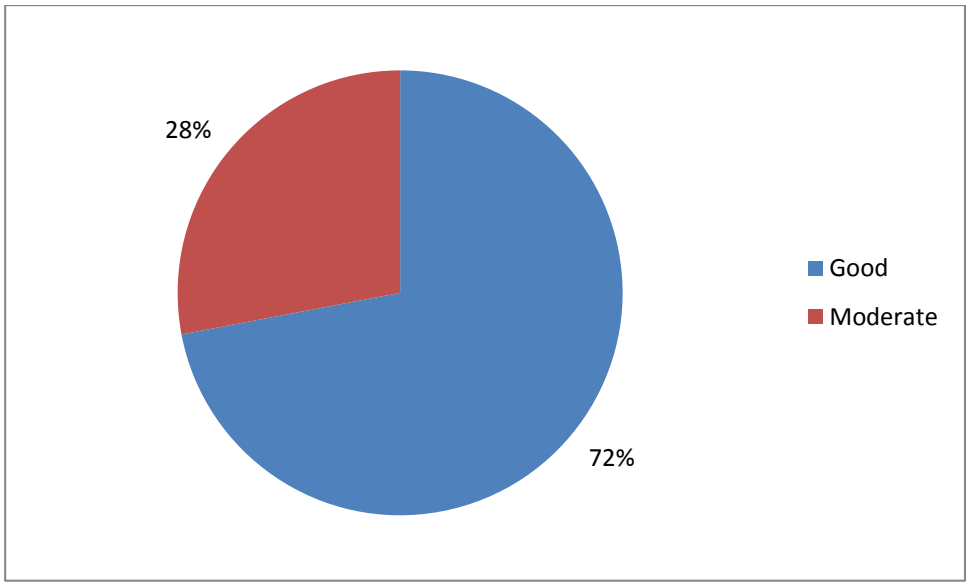

Fig 1 Skeletal preservation

2.2 Truncation

While there was no evidence of recent disturbance to the archaeological levels, three of the later burials were partially disturbed by the bucket of the machine during excavation. Ten inhumations lay only partly within the area of excavation and were thus only partially recovered. Complete recovery of skeletal remains is desirable as they provide more information during osteological analysis. However, it is rare to recover complete remains from archaeological sites and sufficient skeletal material was present to allow systematic sampling for biomolecular analysis.

The pattern of skeletal completeness divided the contexts into two groups, reflecting the nature of the excavation (Fig 2). Those burials located towards the centre of the shaft were generally 50% or more complete, while those at the edges of the shaft tended to be less than 35% complete. As always in osteological studies, true prevalence rates (per bone) provide a far more accurate and representative measure than crude prevalence rates of disease (rates per individual), off-setting to some degree the problems of studying truncated remains.

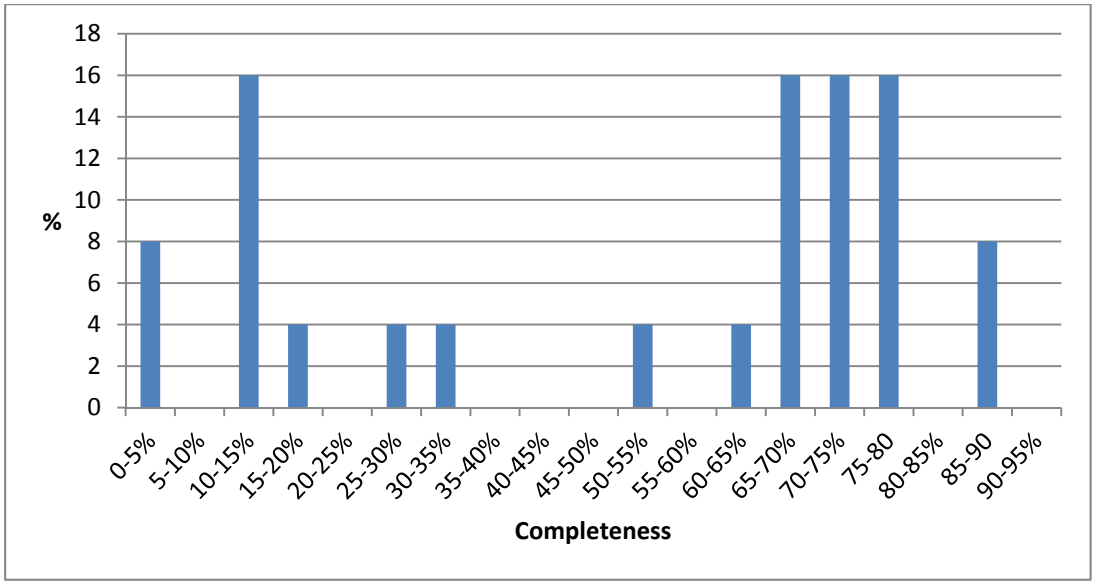

Fig 2 Skeletal completeness

2.3 Sampling

To ensure optimum use of sampled material and keep destruction to a minimum, a phased analytical programme was designed in consultation with relevant specialists. Twelve tooth samples were selected by Dr Sharon DeWitte of the University of South Carolina (Table 1) (Fig 3). The samples were forwarded to Professor Hendrik Poinar of McMaster University Ancient DNA Centre, Hamilton, Ontario, for DNA extraction and screening for Yersinia pestis. Professor Poinar sliced ten of the teeth in half longitudinally and forwarded one half of each to Dr Janet Montgomery at Durham University. Isotope data for these samples was measured by Dr G Nowell of the Department of Earth Sciences at Durham University and A.R. Gledhill and J. Towers of the Department of Archaeological Sciences at the University of Bradford. Data analysis on the strontium, oxygen, carbon and nitrogen isotope samples was then carried out by Dr Montgomery and Dr Julia Beaumont of the University of Bradford. Collagen extracted from five teeth was then sent for radiocarbon dating to the 14CHRONO Centre for Climate, the Environment, and Chronology at Queen's University Belfast.

Context	Phase	Tooth sampled (FDI)	Stable isotope	C14
182	1	14	x	x
185	1	44	x	
188	1	37	x	x
191	1	45		
194	1	38	x	
159	2	38	x	x
134	3	38	x	
137	3	44		
140	3	46	x	x
143	3	27	x	
146	3	48	x	
152	3	24	x	x

Table 1 XTE12 tooth samples sent to Professor Hendrik Poinar (indicating those forwarded for stable isotope analysis and radiocarbon dating)

Fig 3 Don Walker and Dr Sharon DeWitte sampling teeth for biomolecular analysis

A single 5g rib sample from context [156] was also sent for dating.

2.4 Finds

A copper alloy pin, possibly used to fasten a shroud, was found between the knees of 18–25 year old probable male [146] from the latest phase of burial. Two short lengths of copper alloy wire of unknown function were found between the knees of 36–45 year old probable male [149] from the latest phase and 36–45 year old probable male [156] from the second phase of burial. Fourteen flat-headed iron nails were recovered from five of the grave fills from the earliest burial phase. While these are likely to be coffin nails, they are surprisingly few in number (Richardson 2013).

2.5 Staining

Green staining was found on the right hand of ≥46 year old female [131] and on the right foot of 26–35 year old male [188], perhaps the result of disintegrated copper alloy personal adornments or pins, or perhaps inclusions within the grave fill. Reddish brown staining on the right ulna of subadult [197] may reflect the presence of iron nails in the grave fill.

2.6 Other evidence

Pottery from the grave fills of all three burial phases provided a date range of c 1270–1500. Phase 3 also contained pottery with a *terminus post-quem* of 1380, although this may have been intrusive (Blackmore 2014).

3 Methods

All articulated human remains with assigned context numbers were recorded directly onto an Oracle 9i (v9.2.0) relational database system (Connell and Rauxloh 2003) (Powers 2008).

Adult age at death estimates employed a combination of pubic symphysis, auricular surface and sternal rib end morphology, and dental attrition (Brothwell 1981; Iscan et al 1984; 1985; Lovejoy et al 1985; Brooks and Suchey 1990). On this basis, each individual was placed into an age category (Table 2).

Individuals aged below 18 years of age were classed as 'subadults'. Their age was estimated using a combination of long bone diaphyseal growth, stage of epiphyseal fusion and tooth development and eruption (Moorees, Fanning and Hunt 1963(a); 1963(b); Maresh 1970; Gustafson and Koch 1974; Scheuer and Black 2000).

Category	Age group	Description
Subadult	perinatal	inter-uterine/neonate
	1–6 months	early post-neonatal infant
	7–11 months	later post-neonatal infant
	1–5 years	early childhood
	6–11 years	later childhood
	12–17 years	adolescence
Adult	18–25 years	young adult
	26–35 years	early middle adult
	36–45 years	later middle adult
	≥46 years	mature adult
Unclassified	adult	≥18 years
	subadult	<18 years

Table 2 Age at death

The assessment of biological sex was only attempted for adults and was based on a suite of morphological characteristics in the os coxae and skull (Powers 2008). Each adult was assigned to one of the following categories: male, probable male, intermediate, probable female, female, undetermined.

A selection of metric and non-metric data was recorded for all adult skeletons and are stored in the site archive for reference (ibid). The calculation of adult stature employed metric data from the right femur, applying the formulae devised by Trotter (1970).

The diagnosis of pathological conditions followed the procedures set out by Roberts and Connell (2004, 34).

The dental catalogue used the two digit FDI system (Fédération Dentaire Internationale) to identify teeth (FDI 1971).

Where appropriate, skeletal elements from different contexts were matched using size, shape, preservation and colour. Full records were kept of all matches. Disarticulated remains were catalogued in an Excel table with details of age, sex and pathological lesions included. Summary catalogues of both articulated and disarticulated remains are provided in the appendix (1).

4 Results

4.1 Demographic data

Of the 25 articulated individuals recovered from XTE12, 23 were adults and two were subadults. One subadult was aged between 6–11 years at death (context [197]: approximately 8 years of age), the

other 12–17 years (context [185]: approximately 17 years of age). Seventeen adults could be placed into specific age ranges, while 16 (69.6%) were assigned biological sex (Table 3).

Years	Subadult	Male	Probable male	Female	Probable female	Undetermined	Total
6–11	1	0	0	0	0	0	1
12–17	1	0	0	0	0	0	1
18–25	0	3	1	0	1	1	6
26–35	0	2	1	0	0	0	3
36–45	0	1	3	1	0	0	5
≥46	0	1	1	1	0	0	3
Adult	0	0	0	0	0	6	6
Total	**2**	**7**	**6**	**2**	**1**	**7**	**25**

Table 3 Demographic profile

For the purpose of further analysis, probable males were combined with males, and probable females with females. Thirteen males and three females were identified, a ratio of 4.3:1. This appears to be an unusually high proportion of males. The overall sex ratio at the East Smithfield Black Death cemetery was 1.77:1 while that at medieval St Mary Spital was 1.2:1 (Grainger et al 2008, 55; Connell et al 2012, 28). However, as we only have a small snapshot of what was probably a large cemetery, we lack information on variations in spatial distribution patterns.

Although the sample size was small, there was a spread of individuals throughout all the age ranges except for young children and infants (Fig 4). A similar spread was evident in the adult age distribution (Fig 5).

Fig 4 Age at death distribution

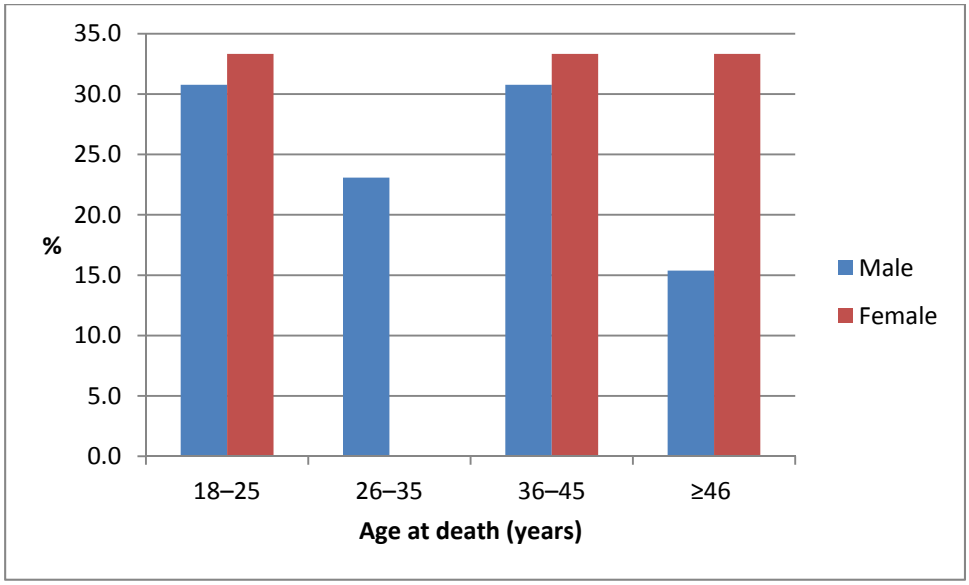

Fig 5 Adult age distribution by sex

4.2 Metric data

4.2.1.1 Stature

Female mean stature was based on a single individual (Table 4). Male mean stature was 172.2cm, within the mean range reported for the late medieval period by Roberts and Cox (2003, 248), but taller than the mean for the East Smithfield Black Death cemetery (168cm) and all periods of medieval burials from St Mary Spital (Grainger et al 2008, 12; Connell et al 2012, 36). However, some caution must be exercised in the interpretation of this result as it is based on such a small sample (8).

	Mean stature	SD	Min.	Max.	n
Female	159.5	-	159.5	159.5	1
Male	172.2	5.3	164.2	174.2	8

Table 4 Stature (cm)

4.2.1.2 Indices

Five adult crania were sufficiently intact to allow measurement of cranial indices (Table 5). The sole female cranium was brachycranic. The four male crania ranged between dolichocranic and brachycranic, with a mesocranic mean.

	Mean	Min.	Max.	n
Male	76.0	70.1	82.9	4
Female	84.4	84.4	84.4	1

Table 5 Cranial index

Lower limb postcranial indices can be used to measure adult diaphyseal morphology (Larsen 1999, 222). The mean platymeric index for females in particular, and the left femora of males, showed a high degree of anteroposterior flattening in the proximal femoral shafts (Table 6). However, the female index was based on only four measurements.

	Left femur	Right femur
Male	82.7	85.5
Female	73.3	76.3

All adults	81.1	83.9

Table 6 Platymeric index (mean)

Mediolateral flattening of the proximal tibial shaft is represented by the platycnemic index. The sole female measurement was mesocnemic (Table 7). The male mean was eurycnemic. The postcranial indices fell within the ranges observed at St Mary Spital (Connell et al 2012, 39).

	Left tibia	Right tibia
Male	73.2	70.3
Female	-	67.9
All adults	72.4	69.8

Table 7 Platycnemic index (mean)

4.3 Non-metric traits

Cranial and postcranial non-metric traits were recorded for all adult skeletons (Table 8) and (Table 9). While some traits have been linked to familial groups and occupational activity, their precise significance is not fully understood (Tyrell 2000). The data reflect morphological information and variation but cannot alone be used to determine relatedness.

Cranial trait	Present		Absent		Total observable		% Prevalance	
Metopism	1		14		15		6.7	
Lambdoid bone	1		10		11		9.1	
Inca bone	0		15		15		-	
Bregmatic bone	0		11		11		-	
Sagittal wormians	1		7		8		12.5	
	Right	**Left**	**Right**	**Left**	**Right**	**Left**	**Right**	**Left**
Asterionic bone	1	1	7	7	8	8	12.5	12.5
Epipteric bone	0	0	8	7	8	7	-	-
Coronal wormians	0	0	9	9	9	9	-	-
Lambdoid wormians	5	3	5	6	10	9	50.0	33.3
Squamo-parietal wormians	0	0	7	7	7	7	-	-
Parietal notch bone	1	1	12	8	13	9	7.7	11.1
Torus auditivi	0	0	15	13	15	13	-	-
Torus maxillaris	0	0	12	12	12	12	-	-
Torus palatinus	0	0	12	12	12	12	-	-
Supraorbital foramen	3	1	9	8	12	9	25.0	11.1
Supraorbital groove	5	4	9	8	14	12	35.7	33.3
Mastoid foramen	5	3	7	7	12	10	41.7	30.0
Foramen of Huschke	0	0	15	13	15	13	-	-
Parietal foramen	3	7	11	7	14	14	50.0	21.4
Accessory infraorbital foramen	0	1	3	3	3	4	-	25.0
Posterior condylar canal	0	0	6	5	6	5	-	-
Multiple mental foramen	0	0	12	12	12	12	-	-
Torus mandibularis	0	0	12	12	12	12	-	-
Mylohyoid bridge	1	0	11	12	12	12	8.3	-

Table 8 Cranial non-metric traits

Post cranial trait	Present		Absent		Total observable		% Prevalence	
Sternal foramen	0		4		4		-	
Manubrio-corpal synostosis	0		13		13		-	
	Right	**Left**	**Right**	**Left**	**Right**	**Left**	**Right**	**Left**
Os acromiale	2	0	10	13	12	13	16.7	-
Acromial articular facet	0	0	12	13	12	13	-	-
Septal aperture	1	1	15	13	16	14	6.3	7.1
Supracondylar process	1	1	16	13	17	14	5.9	7.1
Atlas posterior bridge	1	2	9	6	10	8	10.0	25.0
Atlas lateral bridge	0	0	11	7	11	7	-	-
Atlas transverse foramen bipartite	0	0	11	7	11	7	-	-
Atlas double facet	2	2	10	10	12	12	16.7	16.7
Accessory sacral/iliac facets	1	0	8	10	9	10	11.1	-
Acetabular crease	0	0	15	15	15	15	-	-
Third trochanter	6	4	11	11	15	17	35.3	26.7
Allen's fossa	0	1	15	13	15	14	-	7.1
Hypotrochanteric fossa	6	8	11	9	17	17	35.3	47.1
Patella vastus notch	2	3	7	9	9	12	22.2	25.0
Bipartite patella	0	0	10	12	10	12	-	-
Tibia medial squatting facet	0	0	15	16	15	16	-	-
Tibia lateral squatting facet	4	6	11	11	15	17	26.7	35.3
Calcaneus facet absent	0	0	16	14	16	14	-	-
Calcaneus facet double	8	9	7	5	15	14	53.3	64.3
Talus os trigonum	0	0	14	15	14	15	-	-
Talus facet double	4	3	9	10	13	13	30.8	23.1
Talus squatting facet	3	2	10	12	13	14	23.1	14.3

Table 9 Postcranial non-metric traits

4.4 Stable isotope analysis

Isotope Analysis of the Charterhouse Skeletons

Undertaken on behalf of Crossrail and MOLA

Final report

10th February 2014

Janet Montgomery[1], Julia Beaumont[2], Jacqueline Towers[2], Geoff Nowell[3]

[1]Department of Archaeology, Durham University, Durham DH1 3LE.

[2]Department of Archaeological Sciences, University of Bradford, Bradford, BD7 1DP.

[3]Department of Earth Sciences, Durham University, Durham DH1 3LE.

Summary

1. 10 teeth were submitted for isotope analysis which resulted in 10 strontium and 10 oxygen isotope determinations of enamel and 137 carbon and nitrogen isotope determinations of dentine collagen.
2. All the isotope data commissioned has now been measured at Durham University (Dr. G. Nowell, Earth Sciences) and the University of Bradford (A.R. Gledhill and J. Towers, Archaeological Sciences).
3. Strontium, oxygen, carbon and nitrogen isotope samples and data are documented in Tables 2 and 3, Appendix 1. A summary of the combined interpretations can be found in Table 1.
4. The unused portions of all teeth, and all spare extracted dentine collagen suitable for radiocarbon dating for all teeth, have been returned to MOLA. No samples have been retained by either Durham or Bradford Universities.

CONTENTS

1. INTRODUCTION

Strontium and oxygen isotope analysis of archaeological human remains can provide evidence of their geographical origins (Fricke, O'Neil, and Lynnerup 1995; Bentley 2006). Chemical elements from ingested food and water are incorporated into teeth and bones and because the isotope ratios of elements such as strontium and oxygen vary geographically, these differences can be used to draw conclusions about whether individuals were of local or non-local origin. The source of strontium in the human skeleton is primarily ingested plants and its isotope ratio is controlled by the type of rocks and soils on which food is grown (Bentley 2006). The source of oxygen in the human skeleton is primarily drinking water (and therefore rainwater) and the isotope ratio is controlled by the climate and topography of the region where the rain falls (Fricke, O'Neil, and Lynnerup

1995). We assume that the people we analyse sourced the bulk of their drinking water and

food locally. Tooth enamel, a skeletal tissue which is highly resistant to alteration during life and burial (Wang and Cerling 1994; Trickett et al. 2003;Montgomery, Evans, and Cooper

2007), represents childhood origins and diet.

Carbon and nitrogen isotope analysis of bone or dentine collagen is used to provide evidence of the sources of dietary protein consumed by humans (Schoeninger and DeNiro

1984; Richards and Hedges 1999). Although it is difficult to know with certainty what time of life or what length of time is represented by bone (Hedges et al. 2007; Valentin

2003)dentine, which mineralises in childhood, provides a far higher level of time resolution

(Beaumont et al. 2013; Eerkens, Berget, and Bartelink 2011; Fuller, Richards, and Mays

2003). By measuring a number of small, sequential samples from a single tooth root which forms over a well-constrained period, a dietary sequence of several years can be pieced together and changes identified. This higher resolution method of incremental dentine

analysis is, however, relatively new, and research is still underway to discover what additional evidence of an individual's diet, health and physiological status may be extracted from such profiles (Reitsema 2013; Eerkens and Bartelink 2013; Fahy et al. 2014).

Ten teeth (one M1; three P1; two M2; four M3) were submitted for isotope analysis Appendix 1 Table 2). For three teeth (152, 182, 194), one third to one half of the apical root had already been removed prior to receipt and therefore for these teeth, a shortened time- sequence was produced.

2. METHODS

2.1 Strontium Isotope Analysis of Tooth Enamel

2.1.1. Sample Preparation

Core enamel for strontium isotope analysis was removed from each tooth and mechanically cleaned using tungsten carbide dental tools following the procedure given in Montgomery (2002). Approximately 20 mg of tooth enamel was collected from each individual using a diamond tipped rotary dental saw. All surfaces of the enamel samples were cleaned and polished with a tungsten carbide dental burr to a depth of >100 µm to remove traces of contaminants such as soil and dentine. Cleaned enamel samples were sealed in containers and transferred to the laboratory for further processing.

2.1.2. Measurement

Strontium was separated from the tooth enamel matrix and measured at the Durham Geochemistry Centre at Durham University Earth Sciences Department. The enamel samples were prepared for strontium isotope analysis using column chemistry methods outlined in Charlier et al. (2006). Samples were heated on a hot plate for 20 minutes in 75 µl of 16N HNO_3, the solution was then diluted with 325 µl of MQ H_2O and heated overnight. The

samples were loaded into cleaned and preconditioned columns containing 60 µl of strontium-specific resin. 2x250 µl 3N HNO_3 was passed through to elute the waste, then

2x200 µl MQ H_2O was passed through to elute the strontium, which was collected.

Following the preparation, the size of the ^{86}Sr beam was tested for each sample to assess the strontium concentrations. From this analysis, a dilution factor could be calculated for each sample and each was diluted to yield a beam size of approximately20V ^{88}Sr tomatchthe intensity of the isotopic reference material, NBS987. The strontium samples were taken up in 1 ml of 3% HNO_3 and were analysed by Multi-Collector Inductively Coupled Plasma Mass Spectrometry (MC-ICP-MS) using a Neptune MC-ICP-MS. Samples were introduced into this using an ESI PFA-50 nebuliser and a glass expansion cinnabar micro-cyclonic spraychamber. Instrumental mass bias was corrected for using a $^{88}Sr/^{86}Sr$ ratio of 8.375209 (the reciprocal

of the $^{86}Sr/^{88}Sr$ ratio of 0.1194) and an exponential law. Corrections for interferences from

Rb and Kr on ^{87}Sr and ^{86}Sr were performed using ^{85}Rb and ^{83}Kr as the monitor masses but in all case the intensity of monitor mass was <0.1mV and therefore insignificant. The average

$^{87}Sr/^{86}Sr$ ratio and reproducibility for the international isotope reference material NBS987

during this study was 0.710250±0.000013 (2σ; n=11).

2.2 Oxygen and Carbon Isotope Analysis of Tooth Enamel

2.2.1 Sample Preparation

A diamond dental burr was used to clean the enamel surface and then obtain a sample of powdered enamel (approximately 5-15 mg). The samples were treated following a procedure modified after Sponheimer(1999). Briefly, in order to remove organic matter and exogenous carbonate, they were treated with 1.7 % NaOCl solution for 30 minutes, rinsed

with de-ionised water, treated with 0.1 M acetic acid for ≤ 10 min, and then rinsed once more, before freeze-drying.

2.2.2. Measurement

Enamel samples were measured at the University of Bradford Stable Light Isotope Laboratory. The powdered enamel samples were weighed into septa-capped vials which were loaded into a FinniganGasbench II. The carbonate component of the enamel reacted with phosphoric acid (103 %) at 70 °C to produce CO_2 which was analysed by a Thermo Delta V Advantage mass spectrometer connected to the Gasbench II. The analytical error estimated from the reproducibility of the standards was ± 0.2 ‰ for $\delta^{18}O$ and ± 0.1 ‰ for $\delta^{13}C$. Enamel values were normalised relative to measurements of internal and international

standards. Two replicates were run for each enamel sample from which mean values were calculated.

2.3. Carbon and Nitrogen Isotope Analysis of Dentine Collagen

2.3.1. Sample Preparation

The dentine samples were prepared using method 2 in Beaumont et al. (2013). Teeth were bisected following removal of the enamel and surface debris was removed by air-abrasion. One half of each tooth was demineralised in 0.5M hydrochloric acid at $4^{O}C$ prior to transverse sectioning. Collagen was prepared from each section using the modified Longin method (Brown et al. 1988; O'Connell and Hedges 1999). Sections were rinsed with de- ionised water, placed in sealed microtubes with pH3 acidified water at $70^{O}C$ for 48 hours, allowing the collagen fibrils to denature. The collagen samples were then freeze dried.

2.3.2. Measurement

Collagen was measured for carbon and nitrogen isotopes in duplicate in the University of Bradford Stable Light Isotope Laboratory. Laboratory and international standards were interspersed throughout each analytical run. The dentine samples were combusted in a Thermo Flash EA 1112 and the separated N_2 and CO_2 was introduced to a Delta plus XL via a Conflo III interface. The C:N ratios obtained from each dentine collagen sample are within the range of 2.9 – 3.6 recommended by Ambrose (1993) and 3.1 – 3.5 suggested by Van Klinken (1999). This indicates well-preserved collagen that has not undergone significant diagenetic alteration. The collagen yields from dentine were between 10-19% by weight before demineralization. An approximate age was assigned to each dentine segment as described in Beaumont et al. (2013).

3. RESULTS

The data can be found in Appendix 1 where they are presented in Table 2 (enamel strontium, oxygen and carbon isotopes and mean dentine carbon and nitrogen isotopes) and Table 3 (incremental dentine carbon and nitrogen).

3.1 Strontium and Oxygen Isotope Results

The strontium isotope ($^{87}Sr/^{86}Sr$) data for the ten Charterhouse individuals range from 0.70813 to 0.71372 with a median value of 0.70931and a mean of 0.7098 +/- 0.0015 (1sd). The oxygen isotope ($\delta^{18}O$) data ranges from 25.2 ‰ to 26.6 ‰ and has a median value of 25.9‰ and a mean of 25.9 +/- 0.5 ‰ (1sd). Box and whisker plots compare the strontium (Fig. 1) and oxygen (Fig. 2) isotope data for the ten Charterhouse individuals with results from the Royal Mint Black Death cemetery at East Smithfield, London (Kendall et al. 2013). For strontium isotopes, the Charterhouse skeletons are not significantly higher to the East

Smithfield skeletons at the 95% confidence limit (p> 0.05,1-tailed t-test). For oxygen isotopes, the Charterhouse skeletons are significantly lower than the East Smithfield skeletons at the 99.9% confidence limit (p< 0.001, 1-tailed t-test). There is one clear outlier for strontium isotopes in the Charterhouse group but no outliers for oxygen isotopes.

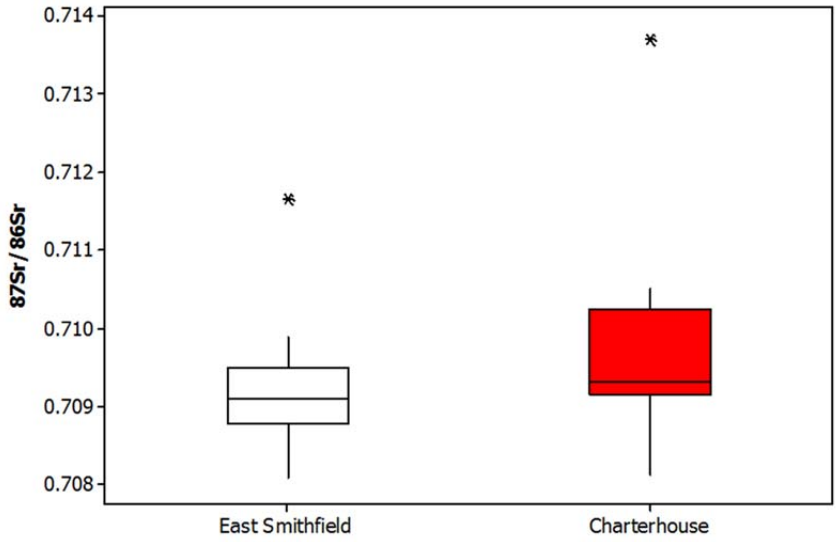

Figure 1. Box and whisker plot for the enamel strontium isotopes measured in the Charterhouse skeletons alongside comparative data from the 14th century AD East Smithfield cemetery (Kendall et al. 2013).

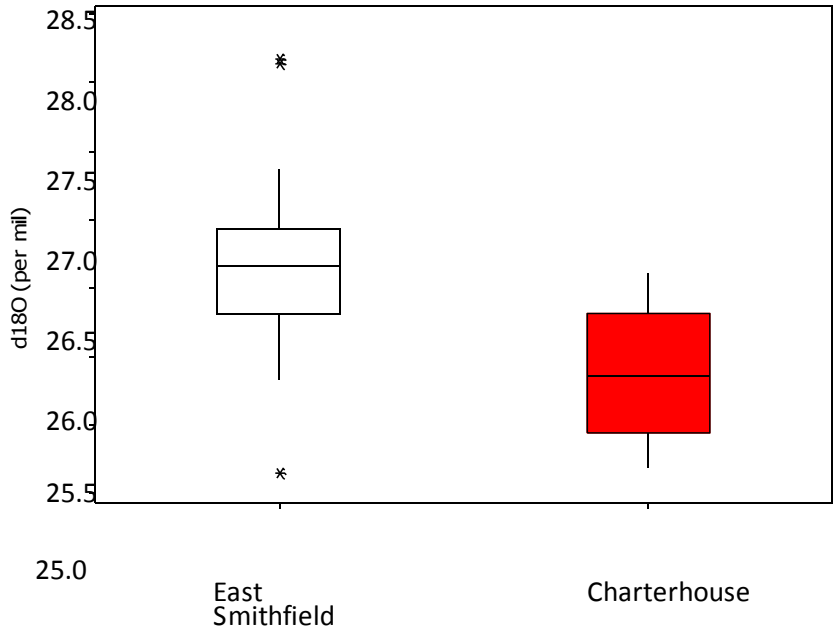

Figure 2. Box and whisker plot for the enamel oxygen isotopes measured in the Charterhouse skeletons alongside comparative data from the 14th century AD East Smithfield cemetery (Kendall et al. 2013).

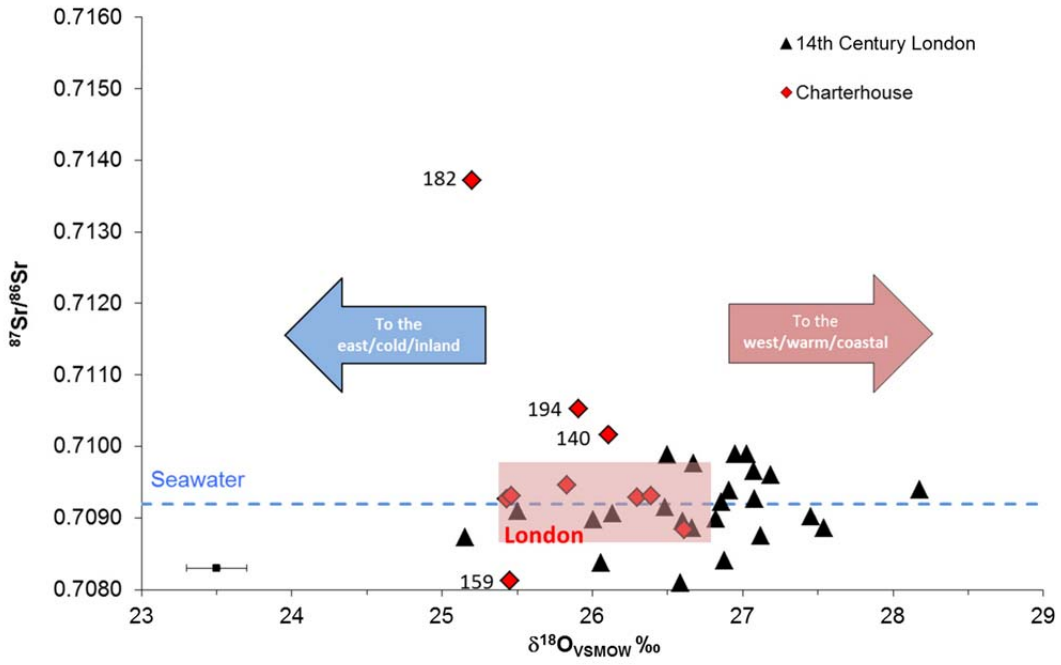

Figure 3. Strontium and oxygen isotope data for the Charterhouse skeletons (red diamonds) compared to 14th Century burials from the East Smithfield cemetery (Kendall et al. 2013).

Figure 3 shows the estimated range (the pale red box) for individuals indigenous to the London area based on the surface geology (London Clay) and oxygen isotopes in precipitation (Evans, Chenery, and Montgomery 2012; Evans et al. 2010). The Charterhouse individuals largely overlap with those from the East Smithfield cemetery but there are no individuals presenting with the high oxygen isotope ratios found at East Smithfield. However, this could be a function of the relatively small sample size (i.e. 10 individuals) in the Charterhouse sample – that is, that there is more variability in the East Smithfield group because it contains more individuals.

3.2 Carbon and Nitrogen Isotope Results

Table 3 in Appendix 1 lists the carbon and nitrogen isotope data measured on dentine collagen. The number of samples per individual varies between 10 and 17 according to the length of the root.Isotope profiles which represent dietary lifeways for each of the ten individuals are displayed in Figure 4 and span the first 23 years of life although the range for each individual is shorter.

The $\delta^{13}C$ values range from -20.1 to -18.1‰ (mean = -19.2 +/- 0.4, 1sd, n = 137); such values in 14thcentury England indicate diets ranging from predominantly terrestrial foods produced in food chain based on C3plants to a mixed diet of terrestrial C_3 and marine foods (Müldner et al. 2009; Müldner and Richards 2005). As can be seen in Figure 4, the majority of individuals produced relatively flat $\delta^{13}C$ profiles indicating negligible change in diet during the period represented by the tooth analysed (e.g. 152, 182, 185). Others show significant changes (14, 143, 188) indicating a diachronic shift in the source of dietary protein. The $\delta^{15}N$ values range from 9.8 to 14.4 ‰ (mean = 12.4 +/- 1.0‰, 1sd, n = 137); such values in 14th century England suggest a variety of diets ranging from one dominated by plants to mixed

diets containing both plant and animal protein (meat or milk) (Müldner and Richards 2005). For some individuals the meat may be a combination of both terrestrial and marine sources (e.g. 156, 159) and one individual appears to have been breastfed during infancy (140). In addition, where the $\delta^{15}N$ profile alone rises, this may, as noted above, be an indication of nitrogen recycling resulting from nutritional or physiological stress (e.g. 146, 185, 194).

Figure 4. (overleaf) A comparison of the carbon and nitrogen isotope profiles for the Charterhouse individuals.

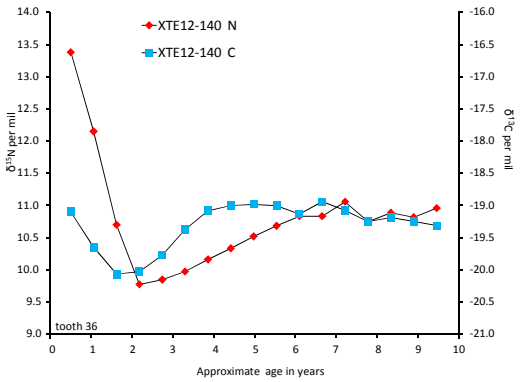
XTE12-140 N
XTE12-140 C
tooth 36
Approximate age in years

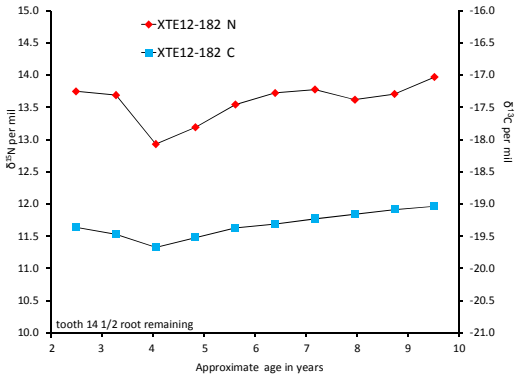
XTE12-182 N
XTE12-182 C
tooth 14 1/2 root remaining
Approximate age in years

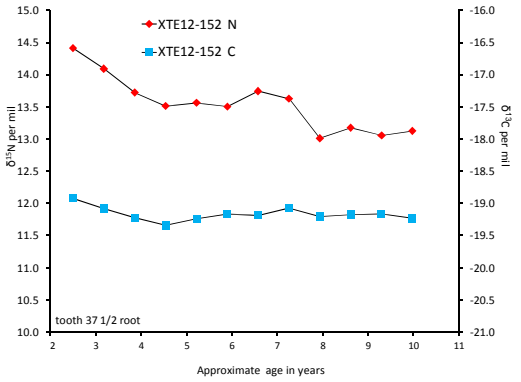
XTE12-152 N
XTE12-152 C
tooth 37 1/2 root
Approximate age in years

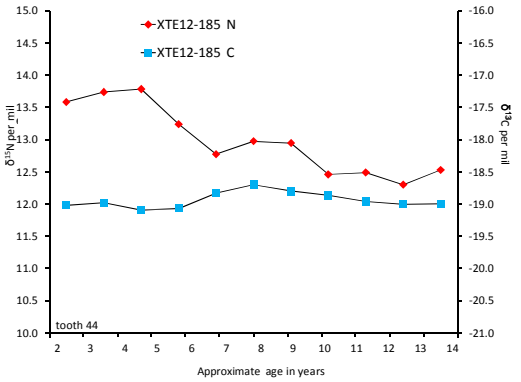
XTE12-185 N
XTE12-185 C
tooth 44
Approximate age in years

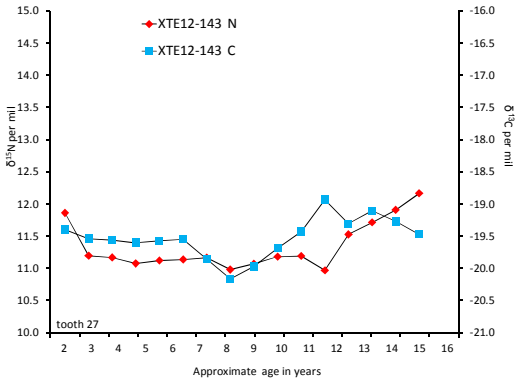
XTE12-143 N
XTE12-143 C
tooth 27
Approximate age in years

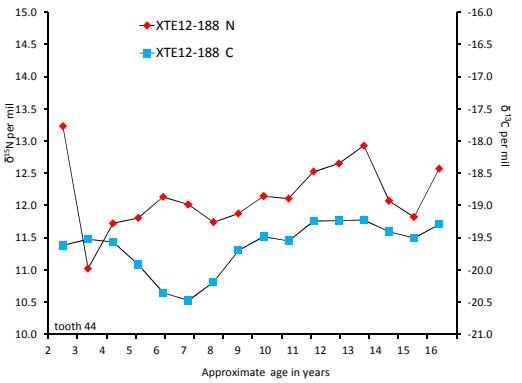
XTE12-188 N
XTE12-188 C
tooth 44
Approximate age in years

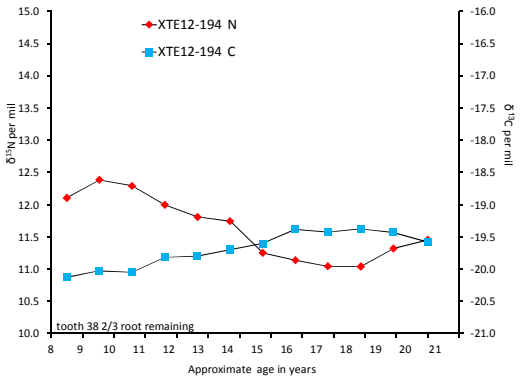
XTE12-194 N
XTE12-194 C
tooth 38 2/3 root remaining
Approximate age in years

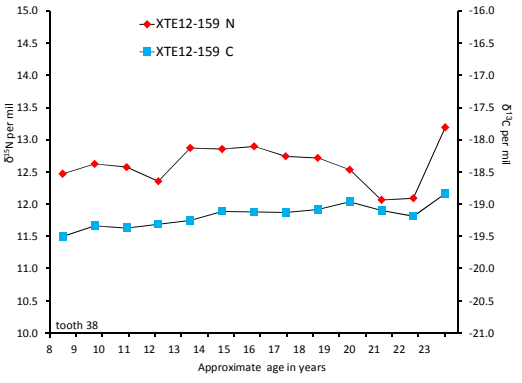
XTE12-159 N
XTE12-159 C
tooth 38
Approximate age in years

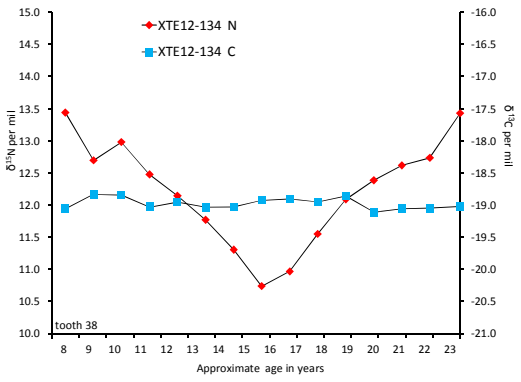
XTE12-134 N
XTE12-134 C
tooth 38
Approximate age in years

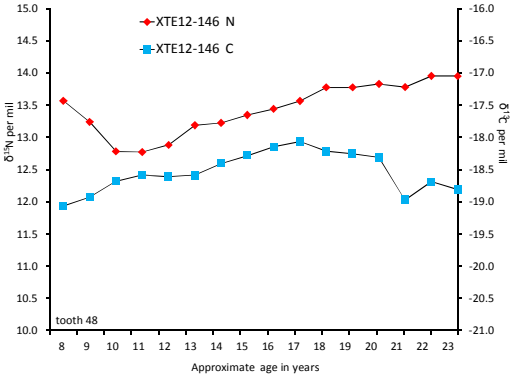
XTE12-146 N
XTE12-146 C
tooth 48
Approximate age in years

4. DISCUSSION

Four individuals (140, 159, 182 and 194) from the Charterhouse site fall outside the estimated London range for strontium isotopes which suggests they moved to London some time after the mineralisation of the measured tooth. In particular:

1. The strontium isotopes for 159 suggest origins on Chalk: this occurs extensively in southern and eastern England but the oxygen isotopes would suggest this individual is more likely to be from the east.

2. Two individuals (140 and 194) have very similar strontium and oxygen isotope ratios – the strontium isotopes are indicative of Mesozoic silicate sediments which occur extensively in southern, central and eastern England(British Geological Survey 2001). Here again, the oxygen isotopes would suggest origins are more likely to be in central or eastern England than the southwest.

3. One individual (182) has a strontium isotope ratio which is high for England and indicative of origins on older Palaeozoic rocks. In Britain, these are primarily found in the southwest, in Wales and in northern England and Scotland. Such values cannot be obtained on the Mesozoic rocks of southern, central and eastern England and the low oxygen isotope ratio would rule out origins in western Britain. If this individual was indigenous, origins in northern Britain or Scotland are most likely.

It should, however, be noted that whilst all the isotope ratios obtained from these individuals could be obtained in Britain, the data cannot prove origins in Britain because

there are many places in the world which will be characterised by comparable isotope values to these.

A summary of residential origins and diet for each individual can be found in Table 1. By combining the mobility data with the high-resolution dietary isotope profiles, further information can be gleaned especially where a change in diet may be linked to a change in residence. For example, individual 159 must have moved to London after the age of c. 16 years and the dietary isotopes suggest a change in diet (increased consumption of marine protein) around the age of 21. Similarly, individual 194 appears to have moved to London in later adolescence and the change of residence appears to be accompanied by a change in diet. It is notable that all but one of the individuals demonstrating isotopic evidence for periods of nutritional or health stress appear to be of local origin. The exception is found in the individual for whomthe only first molar (which is an early-forming tooth)in the sample was submitted for analysis: individal 140 moved to London after the age of c. 5 and after this age, their dietary profile stabilised.

5. CONCLUSIONS

The isotope data shows that the ten individuals investigated from the Charterhouse cemetery were varied in both their residential and dietary histories. Some individuals originated from considerable distances away, providing evidence of migration to the city during the 14th century AD. Moreover, the novel dentine profiling provides significantly enhanced time-resolution of their individual dietary and physiological history on a sub- annual scale. The results show individuals who experienced significant changes both in the source of their food, e.g. breastmilk, meat, plants, marine foods, and their nutritional status with some individuals exhibiting physiological stress as evidenced by nitrogen recycling.

Table 1 Summary interpretation of the combined mobility and dietary isotope data for the Charterhouse skeletons.

Skeleton	Tooth	Origin	Approximate Age Range of Dietary Profile	Dietary Observations
XTE12-182	14	Non-local - moved to London after the age of 8	2.5 to 9.5	No clear change in $\delta^{13}C$ and $\delta^{15}N$values and thus protein type
XTE12-185	44	Consistent with London	2.5 to 13.5	No clear change in $\delta^{13}C$ and thus protein type: possible nutritional/health stress between 2.5 and 5 years of age
XTE12-188	37	Consistent with London	2.5 to 15.5	Significant dietary changes in childhood and period of nutritional/health stress between 4 and 8 years of age
XTE12-194	38	Non-local - moved to London after the age of 16	8.5 to 20	Changes in $\delta^{13}C$ and $\delta^{15}N$ values suggest change in diet, e.g. meat to plant-based which may be contemporaneous with the change of residence after the age of 16
XTE12-159	38	Non-local - moved to London from a Chalk region after the age of 16	8.5 to 23	No change in $\delta^{13}C$ until c.21 years of age when marine protein increases
XTE12-134	38	Consistent with London	8.5 to 23	No change in $\delta^{13}C$ - significant changes in protein type (possibly meat to plant) between 11 and 20 years of age
XTE12-140	46	Non-local - moved to London after the age of 5	birth to 10	Breast fed in infancy coupled with nutritional/health stress. Diet stabilises after the age of 5. Plant-based diet?
XTE12-143	27	Consistent with London	2 to 15	Dietary variation between 6.5 and 11 years of age followed by nutritional and/or health stress between 12 and 15 years of age
XTE12-146	48	Consistent with London	8.5 to 23	Nutritional/health stress from ? To 10 years of age and 17 to 23 years of age? Probable marine protein consumer
XTE12-152	24	Consistent with London	2.5 to 10	No clear change in $\delta^{13}C$ values and thus protein type

6. REFERENCES

AlQahtani, S. J., M. P. Hector, and H. M. Liversidge. 2010. Brief communication: The London atlas of human tooth development and eruption. American Journal of Physical Anthropology 142 (3):481-490.

Ambrose, S. 1993. Isotopic analysis of paleodiets: methodological and interpretive considerations. In Investigations of ancient human tissue: chemical analyses in anthropology, edited by M. K. Sandford. Langhorne: Gordon & Breach Science Publishers.

Beaumont, J., A. Gledhill, J. Lee-Thorp, and J. Montgomery. 2013. Childhood diet: a closer examination of the evidence from dental tissues using stable isotope analysis of incremental human dentine. Archaeometry 55 (2):277-295.

Beaumont, J., A.R. Gledhill, J. Lee-Thorp, and J. Montgomery. 2013. Childhood diet: a closer examination of the evidence from dental tissues using stable isotope analysis of incremental human dentine. Archaeometry 55 (2):277-295.

Bentley, R. A. 2006. Strontium isotopes from the earth to the archaeological skeleton: A review. Journal of Archaeological Method and Theory 13 (3):135-187.

British Geological Survey. 2001. Solid Geology Map UK South Sheet. Southampton: Ordnance Survey/NERC.

Brown, T.A., D.E. Nelson, J.S. Vogel, and J.R. Southon. 1988. Improved collagen extraction by modified Longin method. Radiocarbon 30:171-177.

Charlier, B.L.A., C. Ginibre, D. Morgan, G.M. Nowell, D.G. Pearson, J.P. Davidson, and C.J. Ottley. 2006. Methods for the microsampling and high-precision analysis of strontium and rubidium isotopes at single crystal scale for petrological and geochronological applications. Chemical Geology.

Eerkens, Jelmer W., and Eric J. Bartelink. 2013. Sex-biased weaning and early childhood diet among middle holocene hunter–gatherers in Central California. American Journal of Physical Anthropology 152 (4):471-483.

Eerkens, Jelmer W., Ada G. Berget, and Eric J. Bartelink. 2011. Estimating weaning and early childhood diet from serial micro-samples of dentin collagen. Journal of Archaeological Science 38 (11):3101-3111.

Evans, J., C.A. Chenery, and J. Montgomery. 2012. A summary of strontium and oxygen isotope variation in archaeological human tooth enamel excavated from Britain. Journal of Analytical Atomic Spectroscopy 27:754-764.

Evans, J.A., J. Montgomery, G. Wildman, and N. Boulton. 2010. Spatial variations in biosphere $^{87}Sr/^{86}Sr$ in Britain. Journal of the Geological Society 167 (1):1-4.

Fahy, Geraldine E., Michael P. Richards, Benjamin T. Fuller, Tobias Deschner, Jean-Jacques Hublin, and Christophe Boesch. 2014. Stable nitrogen isotope analysis of dentine serial sections elucidate sex differences in weaning patterns of wild chimpanzees (Pan troglodytes). American Journal of Physical Anthropology:n/a-n/a.

Fricke, Henry C., James R. O'Neil, and Niels Lynnerup. 1995. Oxygen isotope composition of human tooth enamel from Medieval Greenland: linking climate and society. Geology 23 (10):869-872.

Fuller, B.T, M. Richards, and S.A Mays. 2003. Stable Carbon and Nitrogen Isotope Variations in Tooth Dentine Serial Sections from Wharram Percy. Journal of Archaeological Science 30:1673-1684.

Hedges, R. E. M., J. G. Clement, C. D. L. Thomas, and T. C. O'Connell. 2007. Collagen turnover in the adult femoral mid-shaft: Modeled from anthropogenic radiocarbon tracer measurements. American Journal of Physical Anthropology 133 (2):808-816.

Kendall, E., J Montgomery, J. Evans, C. Stantis, and V. Mueller. 2013. Mobility, Mortality, and the Middle Ages: Identification of Migrant Individuals in a 14th Century Black Death Cemetery Population. American Journal of Physical Anthropology 150 (2):210-22.

Montgomery, J, JA Evans, and RE Cooper. 2007. Resolving archaeological populations with Sr-isotope mixing models. Applied Geochemistry 22 (7):1502-1514.

Montgomery, Janet. 2002. Lead and Strontium Isotope Compositions of Human Dental Tissues as an Indicator of Ancient Exposure and Population Dynamics. Archaeological Sciences.

Müldner, G., and M. P. Richards. 2005. Fast or feast: reconstructing diet in later Medieval England by stable isotope analysis. Journal of Archaeological Science 32:39-48.

Müldner, Gundula, Janet Montgomery, Gordon Cook, Rob Ellam, Andrew Gledhill, and Chris Lowe. 2009. Isotopes and individuals: diet and mobility among the medieval Bishops of Whithorn. Antiquity 83 (322):1119-1133.

O'Connell, T. C., and R. E. M. Hedges. 1999. Isotopic Comparison of Hair and Bone: Archaeological Analyses. Journal of Archaeological Science 26 (6):661-665.

Reitsema, Laurie J. 2013. Beyond diet reconstruction: Stable isotope applications to human physiology, health, and nutrition. American Journal of Human Biology 25 (4):445-456.

Richards, M.P., and R.E.M. Hedges. 1999. A Neolithic revolution? New evidence of diet in the British Neolithic. Antiquity 73:891-897.

Schoeninger, M. J., and M. J. DeNiro. 1984. Nitrogen and carbon isotopic composition of bone collagen from marine and terrestrial animals. Geochimica et Cosmochimica Acta 48:625-639.

Sponheimer, M. 1999. Isotopic ecology of the Makapansgat Limeworks fauna, Graduate School, New Brunswick, Rutgers, The State University of New Jersey.

Trickett, M. A., P. Budd, J. Montgomery, and J. Evans. 2003. An assessment of solubility profiling as a decontamination procedure for the Sr-87/Sr-86 analysis of archaeological human skeletal tissue. Applied Geochemistry 18 (5):653-658.

Valentin, J., ed. 2003. Basic Anatomical and Physiological Data for Use in Radiological Protection: Reference Values. Vol. ICRP Publication 89, Annals of the ICRP: International Commission on Radiological Protection.

VanKlinken, G. J. 1999. Bone collagen quality indicators for palaeodietary and radiocarbon measurements. Journal of Archaeological Science 26 (6):687-695.

Wang, Y., and T.E. Cerling. 1994. A model of fossil tooth and bone diagenesis: implications for paleodiet reconstruction from stable isotopes. Palaeogeography, Palaeoclimatology, Palaeoecology 107 (3-4):281-289.

APPENDIX 1.

Isotope Data Tables

Table 2.Bulk isotope data for the Charterhouse teeth. Note: dentine values are the means of the individual measurements made on each tooth root (n is variable) which are detailed in Table 3.

		Laboratory Tissue	Durham Enamel	Bradford Enamel	Bradford Enamel	Bradford Mean Dentine	Bradford Mean Dentine
Skeleton	Lab code	Tooth	$^{87}Sr/^{86}Sr$	$\delta^{18}O$ ‰	$\delta^{13}C$ ‰	$\delta^{13}C$ ‰	$\delta^{15}N$ ‰
XTE12-182	HP2268	14	0.713718	25.2	-12.9	-19.3	13.6
XTE12-185	HP2269	44	0.709314	26.4	-12.8	-18.9	13.0
XTE12-188	HP2270	37	0.709312	25.5	-12.6	-19.6	12.1
XTE12-194	HP2272	38	0.710523	25.9	-13.2	-19.7	11.6
XTE12-159	HP2273	38	0.708129	25.5	-12.6	-19.2	12.6
XTE12-134	HP2274	38	0.709462	25.8	-12.7	-19.0	12.2
XTE12-140	HP2276	46	0.710162	26.1	-13.9	-19.3	10.8
XTE12-143	HP2277	27	0.708834	26.6	-13.4	-19.5	11.3
XTE12-146	HP2278	48	0.709266	25.4	-13.5	-18.5	13.4
XTE12-152	HP2279	24	0.709287	26.3	-13.2	-19.2	13.5

Table3.Incremental carbon and nitrogen isotope data from dentine collagen. Analyses are mean values of duplicate measurements. Estimated age in years for each sample was calculated followingAlQahtaniet al. (2010) and Beaumont et al. (2013).

Skeleton	Lab Code	$\delta^{15}N$	$\delta^{13}C$	Amt%C	Amt%N	C:N	Age in Years
XTE12-182	HP2268-1	13.7	-19.4	41.4	15.1	3.2	2.5
	HP2268-2	13.7	-19.5	41.9	15.3	3.2	3.3
	HP2268-3	12.9	-19.7	41.5	15.0	3.2	4.1
	HP2268-4	13.2	-19.5	41.3	15.0	3.2	4.8
	HP2268-5	13.5	-19.4	41.5	15.0	3.2	5.6
	HP2268-6	13.7	-19.3	41.8	15.1	3.2	6.4
	HP2268-7	13.8	-19.2	41.5	15.0	3.2	7.2
	HP2268-8	13.6	-19.2	41.4	15.0	3.2	8.0
	HP2268-9	13.7	-19.1	41.5	15.0	3.2	8.7
	HP2268-10	14.0	-19.0	41.1	14.8	3.2	9.5
	Mean	13.6	-19.3				
XTE12-185	HP2269-1	13.6	-19.0	41.0	14.9	3.2	2.5
	HP2269-2	13.7	-19.0	40.7	14.8	3.2	3.6
	HP2269-3	13.8	-19.1	41.0	15.0	3.2	4.7
	HP2269-4	13.2	-19.1	41.0	14.9	3.2	5.8
	HP2269-5	12.8	-18.8	40.9	14.9	3.2	6.9
	HP2269-6	13.0	-18.7	40.7	14.8	3.2	8.0
	HP2269-7	12.9	-18.8	41.0	15.0	3.2	9.1
	HP2269-8	12.5	-18.9	40.8	14.9	3.2	10.2
	HP2269-9	12.5	-19.0	41.1	15.0	3.2	11.3
	HP2269-10	12.3	-19.0	39.2	14.3	3.2	12.4
	HP2269-11	12.5	-19.0	40.9	14.9	3.2	13.5
	Mean	13.0	-18.9				
XTE12-194	HP2272-1	12.1	-20.1	40.6	14.9	3.2	8.5
	HP2272-2	12.4	-20.0	40.8	15.0	3.2	9.6
	HP2272-3	12.3	-20.0	40.9	15.0	3.2	10.7
	HP2272-4	12.0	-19.8	41.0	15.1	3.2	11.8
	HP2272-5	11.8	-19.8	40.7	14.9	3.2	12.9
	HP2272-6	11.7	-19.7	40.4	14.7	3.2	14.0
	HP2272-7	11.3	-19.6	41.1	15.0	3.2	15.1
	HP2272-8	11.1	-19.4	41.2	15.0	3.2	16.2
	HP2272-9	11.0	-19.4	41.2	15.1	3.2	17.3
	HP2272-10	11.0	-19.4	41.0	15.1	3.2	18.4
	HP2272-11	11.3	-19.4	41.0	15.0	3.2	19.5
	HP2272-12	11.5	-19.6	40.6	14.8	3.2	20.6
	Mean	11.6	-19.7				

Skeleton	Lab Code	$\delta^{15}N$	$\delta^{13}C$	Amt%C	Amt%N	C:N	Age in Years
XTE12-159	HP2273-1	12.5	-19.5	15.6	42.1	3.2	8.5
	HP2273-2	12.6	-19.3	15.8	42.6	3.2	9.6
	HP2273-3	12.6	-19.4	15.6	42.5	3.2	10.7
	HP2273-4	12.4	-19.3	15.9	43.0	3.2	11.8
	HP2273-5	12.9	-19.3	15.7	42.4	3.1	12.9
	HP2273-6	12.9	-19.1	15.7	42.5	3.2	14.1
	HP2273-7	12.9	-19.1	15.6	42.4	3.2	15.2
	HP2273-8	12.7	-19.1	15.6	42.4	3.2	16.3
	HP2273-9	12.7	-19.1	15.6	42.1	3.2	17.4
	HP2273-10	12.5	-19.0	15.4	41.8	3.2	18.5
	HP2273-11	12.1	-19.1	15.5	41.9	3.2	19.6
	HP2273-12	12.1	-19.2	15.2	41.7	3.2	20.7
	HP2273-13	13.2	-18.8	15.0	41.5	3.2	21.8
	Mean	12.6	-19.2				
XTE12-152	HP2279-1	14.4	-18.9	15.8	42.8	3.2	2.5
	HP2279-2	14.1	-19.1	16.0	42.8	3.1	3.2
	HP2279-3	13.7	-19.2	16.0	42.9	3.1	3.9
	HP2279-4	13.5	-19.3	15.9	43.0	3.1	4.5
	HP2279-5	13.6	-19.2	16.1	43.1	3.1	5.2
	HP2279-6	13.5	-19.2	15.9	42.9	3.1	5.9
	HP2279-7	13.7	-19.2	15.9	42.7	3.1	6.6
	HP2279-8	13.6	-19.1	15.9	42.8	3.1	7.3
	HP2279-9	13.0	-19.2	15.8	42.7	3.2	7.9
	HP2279-10	13.2	-19.2	15.9	42.8	3.1	8.6
	HP2279-11	13.1	-19.2	15.9	42.9	3.2	9.3
	HP2279-12	13.1	-19.2	15.8	42.5	3.1	10.0
	Mean	13.5	-19.2				
XTE12-188	HP2270-1	13.2	-19.6	15.8	42.6	3.1	2.5
	HP2270-2	11.0	-19.5	15.8	42.7	3.2	3.4
	HP2270-3	11.7	-19.6	16.0	42.9	3.1	4.2
	HP2270-4	11.8	-19.9	15.7	42.6	3.2	5.1
	HP2270-5	12.1	-20.4	15.9	42.6	3.1	5.9
	HP2270-6	12.0	-20.5	15.9	42.9	3.1	6.8
	HP2270-7	11.7	-20.2	15.8	42.7	3.1	7.7
	HP2270-8	11.9	-19.7	15.9	42.6	3.1	8.5
	HP2270-9	12.1	-19.5	15.7	42.9	3.2	9.4
	HP2270-10	12.1	-19.6	15.9	42.8	3.1	10.2
	HP2270-11	12.5	-19.2	15.9	42.7	3.1	11.1
	HP2270-12	12.7	-19.2	15.9	42.9	3.1	12.0
	HP2270-13	12.9	-19.2	15.8	42.7	3.1	12.8
	HP2270-14	12.1	-19.4	15.8	42.7	3.1	13.7
	HP2270-15	11.8	-19.5	15.8	42.8	3.2	14.5
	HP2270-16	12.6	-19.3	15.7	42.6	3.2	15.4
	Mean	12.1	-19.6				

Skeleton	Lab Code	$\delta^{15}N$	$\delta^{13}C$	Amt%C	Amt%N	C:N	Age in Years
XTE12-140	HP2276-1	13.4	-19.1	15.2	41.5	3.2	0.5
	HP2276-2	12.1	-19.7	15.4	41.9	3.2	1.1
	HP2276-3	10.7	-20.1	15.4	41.9	3.2	1.6
	HP2276-4	9.8	-20.0	15.6	42.0	3.2	2.2
	HP2276-5	9.8	-19.8	15.3	41.7	3.2	2.7
	HP2276-6	10.0	-19.4	15.4	41.8	3.2	3.3
	HP2276-7	10.2	-19.1	15.5	41.9	3.2	3.9
	HP2276-8	10.3	-19.0	15.4	41.9	3.2	4.4
	HP2276-9	10.5	-19.0	15.4	41.8	3.2	5.0
	HP2276-10	10.7	-19.0	15.4	41.7	3.2	5.5
	HP2276-11	10.8	-19.1	15.4	41.9	3.2	6.1
	HP2276-12	10.8	-18.9	15.4	41.7	3.2	6.7
	HP2276-13	11.1	-19.1	15.3	41.7	3.2	7.2
	HP2276-14	10.7	-19.3	15.2	41.4	3.2	7.8
	HP2276-15	10.9	-19.2	15.2	41.4	3.2	8.3
	HP2276-16	10.8	-19.3	15.4	41.8	3.2	8.9
	HP2276-17	11.0	-19.3	15.3	41.7	3.2	9.5
	Mean	10.8	-19.3				
XTE12-134	HP2274-1	13.4	-19.1	15.5	41.7	3.1	8.5
	HP2274-2	12.7	-18.8	15.4	41.6	3.2	9.5
	HP2274-3	13.0	-18.8	15.5	41.6	3.1	10.6
	HP2274-4	12.5	-19.0	15.5	41.7	3.1	11.6
	HP2274-5	12.1	-19.0	15.4	41.6	3.2	12.6
	HP2274-6	11.8	-19.0	15.4	41.7	3.2	13.7
	HP2274-7	11.3	-19.0	15.5	41.8	3.1	14.7
	HP2274-8	10.7	-18.9	15.5	42.1	3.2	15.7
	HP2274-9	11.0	-18.9	15.5	42.0	3.2	16.7
	HP2274-10	11.6	-19.0	15.6	42.1	3.2	17.8
	HP2274-11	12.1	-18.9	15.5	41.8	3.1	18.8
	HP2274-12	12.4	-19.1	15.5	41.8	3.1	19.8
	HP2274-13	12.6	-19.1	15.5	41.8	3.2	20.9
	HP2274-14	12.7	-19.0	15.4	41.6	3.2	21.9
	HP2274-15	13.4	-19.0	15.4	41.7	3.2	22.9
	Mean	12.2	-19.0				

Skeleton	Lab Code	$\delta^{15}N$	$\delta^{13}C$	Amt%C	Amt%N	C:N	Age in Years
XTE12-143	HP2277-1	11.9	-19.4	15.1	41.5	3.2	2.5
	HP2277-2	11.2	-19.5	15.3	42.3	3.2	3.3
	HP2277-3	11.2	-19.6	15.2	41.7	3.2	4.1
	HP2277-4	11.1	-19.6	15.4	42.2	3.2	4.9
	HP2277-5	11.1	-19.6	15.3	42.1	3.2	5.7
	HP2277-6	11.1	-19.5	15.4	42.2	3.2	6.6
	HP2277-7	11.2	-19.9	15.5	42.3	3.2	7.4
	HP2277-8	11.0	-20.2	15.5	41.8	3.1	8.2
	HP2277-9	11.1	-20.0	15.4	42.2	3.2	9.0
	HP2277-10	11.2	-19.7	15.7	42.6	3.2	9.8
	HP2277-11	11.2	-19.4	15.4	42.0	3.2	10.6
	HP2277-12	11.0	-18.9	15.4	41.9	3.2	11.4
	HP2277-13	11.5	-19.3	15.4	41.8	3.2	12.2
	HP2277-15	11.7	-19.1	15.3	42.1	3.2	13.0
	HP2277-16	11.9	-19.3	15.4	42.0	3.2	13.8
	HP2277-17	12.2	-19.5	15.0	41.4	3.2	14.7
	Mean	11.3	-19.5				
XTE12-146	HP2278-1	13.6	-19.1	15.2	41.9	3.2	8.5
	HP2278-2	13.2	-18.9	15.6	43.1	3.2	9.5
	HP2278-3	12.8	-18.7	15.6	42.7	3.2	10.4
	HP2278-4	12.8	-18.6	15.3	42.0	3.2	11.4
	HP2278-5	12.9	-18.6	15.8	43.3	3.2	12.4
	HP2278-6	13.2	-18.6	15.1	41.7	3.2	13.3
	HP2278-7	13.2	-18.4	15.2	42.0	3.2	14.3
	HP2278-8	13.3	-18.3	15.2	41.9	3.2	15.3
	HP2278-9	13.4	-18.1	15.4	42.3	3.2	16.2
	HP2278-10	13.6	-18.1	15.3	42.0	3.2	17.2
	HP2278-11	13.8	-18.2	15.0	41.8	3.2	18.2
	HP2278-12	13.8	-18.3	15.0	41.7	3.2	19.1
	HP2278-13	13.8	-18.3	15.2	42.4	3.2	20.1
	HP2278-14	13.8	-19.0	15.2	41.9	3.2	21.1
	HP2278-15	14.0	-18.7	14.7	41.6	3.3	22.0
	HP2278-16	14.0	-18.8	14.7	41.9	3.3	23.0
	Mean	13.4	-18.5				

4.5 Radiocarbon dating

Following a dating simulation exercise, Baysian modelling was applied to six calibrated (OxCal 4.2) radiocarbon dates obtained by the 14CHRONO Centre for Climate, the Environment, and Chronology at Queen's University Belfast (Ruddy 2014). The model indicated that the stratigraphy, radiocarbon dates and pottery data were consistent and reliable. The first two phases of burial were dated to the 14th century and may well have been contemporary with the 1348/9 plague (Table 10). It is also possible that some or all of the burials may have come from a slightly later outbreak of plague, such as the Pestis Secunda (1361–2). The phase 3 burials probably date to the 15th century.

Laboratory code	Radiocarbon determination	Calibrated date (cal AD, 95.4% probability)	Modelled date (cal AD, 95.4% probability)	Phase
UBA-24641	605±18	1299 to 1370 (75.1%) 1380 to 1403 (20.3%)	1304 to 1388 (95.4%)	1
UBA-24642	672±20	1276 to 1310 (58.3%) 1360 to 1388 (37.1%)	1280 to 1309 (28.7%) 1354 to 1386 (66.7%)	
UBA-24640	645±20	1285 to 1320 (40.1%) 1350 to 1392 (55.3%)	1356 to 1396 (95.4%)	2
UBA-24650	425±21	1432AD (95.4%) 1486AD	1430 to 1474 (95.4%)	3
UBA-24653	517±23	1333 to 1336 (1.0%) 1398 to 1441 (94.4%)	1400 to 1439 (95.4%)	

Table 10 Summary of calibrated and modelled radiocarbon dates

4.6 Palaeopathology

4.6.1 Dental disease

Data for dental pathology was analysed by individual (crude prevalence) (Table 11), by tooth for caries, calculus and enamel hypoplasia, and by tooth socket for periodontal disease and periapical lesions (true prevalence) (Table 12) (Table 13).

	Subadults			Adults			Total		
	n	**Affected**	**%**	**n**	**Affected**	**%**	**n**	**Affected**	**%**
Caries	2	2	100	23	7	30.4	25	9	36.0
Calculus		2	100		11	47.8		13	52.0
Enamel hypoplasia		0	-		5	21.7		5	20.0
Periodontal disease		1	50		9	39.1		10	40
Periapical lesion		0	-		4	17.4		4	16.0

Antemortem loss		1	50		7	30.4		8	32.0

Table 11 Dental pathology crude prevalence

	Deciduous			Permanent			Total		
	n	**Affected**	**%**	**n**	**Affected**	**%**	**n**	**Affected**	**%**
Caries	7	1	14.3	33	2	6.1	40	3	7.5
Calculus		1	14.3		26	78.8		27	67.5
Enamel hypoplasia		0	-		0	-		0	-
Periodontal disease	5	0	-	48	5	10.4	53	5	9.4
Periapical lesion		0	-		0	-		0	-

Table 12 Subadult dental pathology true prevalence

	Permanent		
	n	**Affected**	**%**
Caries	296	14	4.7
Calculus		186	62.8
Enamel hypoplasia		19	6.4
Periodontal disease	367	115	31.3
Periapical abscess		7	1.9

Table 13 Adult dental pathology true prevalence

More than one third of individuals had dental caries (9/25: 36%), cavities caused by acid-forming bacteria, often the result of the consumption of sugary and starchy foods (Hillson 1996, 269, 278–83). The true prevalence rate of adult caries (14/296: 4.7%) was lower than that observed at St Mary Spital (period 16 4047/39,143: 10.3%) (Connell et al 2012, 42–3), suggesting those buried at Charterhouse had a better level of dental health, and possibly a lower sugar consumption. Individual [140], an 18–25 year old male, was particularly badly affected, with six carious teeth (Fig 6).

Fig 6 Dental caries in maxillae of XTE12 [140] (temporary image)

Corrected caries (below): incorrect calculations used: see P:\MULTI\1051\XTE12\Env\PXA Charterhouse\Human bone\Archive\Dental for correct version

As carious teeth can be lost prior to death ('ante-mortem tooth loss') the true prevalence of caries may underestimate the actual rate in older age groups. In order to rectify this, a 'corrected' caries rate is calculated by adding the ante-mortem tooth loss rate to the caries rate (Table 14) (Fig 7).

Age (years)	n	Carious teeth	%	Ante-mortem loss	Ante-mortem loss %	Corrected caries %
18–25	147	8	5.4	2	1.3	6.7
26–35	103	2	1.9	0	-	1.9
36–45	90	4	4.4	15	11.5	15.9

≥46	25	0	-	10	8.7	8.7

Table 14 Calculation of corrected caries rate

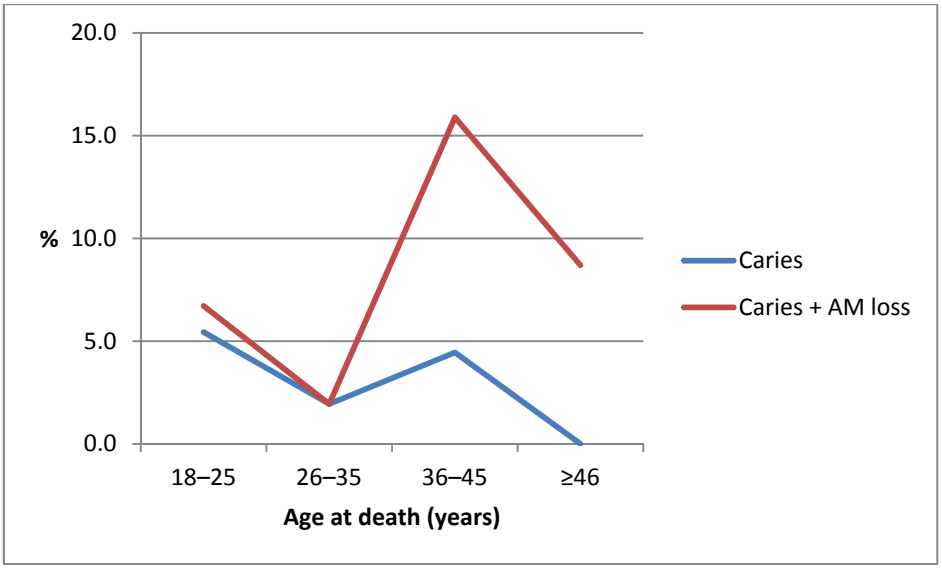

Fig 7 Comparison of caries and corrected caries rates by age

Periapical lesions were present in the dentitions of 4 adult individuals (/23: 17.4%) and in 1.9% (7/367) of adult tooth positions. Three of the seven lesions were associated with individual [140] who was also severely affected by caries (Fig 8). A particularly large lesion had developed by the time 36–45 year old male [152] died (Fig 9).

Fig 8 Periapical lesion in left mandible of XTE12 [140] (temporary image)

Fig 9 Periapical lesion in right maxilla of XTE12 [152] (temporary image)

Thirteen individuals (/25: 52%) had dental calculus deposits, though only 16 had dentitions (13/16: 81.2%). This is mineralised plaque that can accumulate on poorly cleaned teeth. It may in some cases also be associated with a carbohydrate-rich diet (Hillson 1996, 259–60). At East Smithfield, the crude prevalence of calculus for adults was very high (94.7%) (Grainger et al 2008, 47–55). The adult sample from Charterhouse Square has a similar high true prevalence rate of calculus, though lower than the prevalence observed at St Mary Spital (period 16: 83.9%) (Connell et al 2012 42–3).

Periodontal disease, the horizontal loss of alveolar bone surrounding the teeth may be hastened by high rates of calculus. This form of gum disease may eventually result in tooth loss, and healing of bone at absent tooth locations can make diagnosis difficult (Hillson 1996, 265). At Charterhouse Square, 39.1% (9/23) of adults were affected, compared to 60.8% (144/237) at East Smithfield (Grainger et al 2008, 47–8, 52–3, 54–5).

Enamel hypoplasia is the term applied to lines and defects of arrested growth in the teeth which reflect episodes of stress resulting from illness or malnutrition during childhood (Aufderheide and Rodríguez-Martín 1998, 405). Five adults contained enamel hypoplastic lesions (/23: 21.7%). Only one of the affected individuals was over the age of 35 years at death, and all came from phases two and three of the cemetery (Table 15).

Phase	n	Affected	%
1	11	0	-
2	2	1	50.0
3	12	4	33.3

Table 15 Enamel hypoplasia crude prevalence by cemetery phase

East Smithfield had a much higher crude prevalence rate of enamel hypoplasia (193/245: 78.8% ($\chi^2 = 35.45$, df = 1, $p \leq 0.0001$)) (Grainger et al 2008, 47–55), although the sample size from Charterhouse Square is relatively small.

4.6.1.1 Dental anomalies

Both subadults [185] and [197] had Carabelli cusps on their maxillary first molars. One pegged third molar was observed in the right maxilla of 18–25 year old male [159], and a shovel-shaped maxillary central incisor in a male from the same age category [140]. Three individuals had dental crowding, all in the mandibular canines, while four individuals were affected by tooth rotation, two in the maxillae and two in the mandible.

4.6.2 Congenital anomalies

4.6.2.1 Spinal disorders

Nine individuals (9/25: 36%) displayed minor congenital anomalies in the form of 12 vertebral border shifts (Powers 2008, 64–8 (after Barnes 1994)). Six of these involved cranial shifts at the thoracolumbar border including five 11th thoracic vertebrae with transitional facets and one hypoplastic 12th rib. Four lumbosacral border shifts were present, four cranial and one caudal. The two sacrocaudal shifts were both caudal and involved sacralisation.

Thirteen individuals (13/25: 52%) contained a total of 27 examples of neural arch non-union, one from the 5th lumbar vertebra and the remainder from the sacrum. Full spina bifida occulta

was present in the spine of 18–25 year old probable male [146]. Occulta is a mild form of spina bifida and is usually asymptomatic (Aufderheide and Rodríguez-Martín 1998, 61).

One example of slight idiopathic scoliosis (curvature of the spine) was observed in the lower thoracic and upper lumbar spines of a 12–17 year old from the first burial phase. The right sides of the vertebral bodies in the lower thoracic spine, and the left sides of the upper lumbar spine were wedged. This form of scoliosis is most commonly discovered in children between 10 and 12 years of age (Aufderheide and Rodríguez-Martín 1998, 66).

Mature adult male [128] had a bifurcated rib (Barnes 1994, 72). He had also suffered bilateral spondylolysis of the fourth lumbar vertebra which has been linked to activity related trauma, perhaps acting on a congenital predisposition (Merbs 1983, 35; Bridges 1989, 328).

A number of segmentation anomalies were observed in the vertebral column of young adult male [134], including hypoplasia of the right transverse process of the first thoracic vertebra, apophyseal hypoplasia in the right inferior fifth lumbar vertebra and right superior first sacral vertebra (Fig 10). The neural arch of a sacralised sixth lumbar vertebra was present but bifurcated due to developmental delay, causing the right half of the lamina and transverse process to separate from the remainder of the bone (Fig 11). This was likely the result of a combined segmental border shift and unilateral hypoplasia (Barnes 1994, 78, 119, 126).

Fig 10 Vertebral bifurcation, hypoplasia and border shift in XTE12 [134] (temporary image)

Fig 11 Vertebral bifurcation, hypoplasia and border shift in XTE12 [134], with separated fragment of sacralised sixth lumbar vertebra removed (temporary image)

4.6.3 Infectious disease

4.6.3.1 Non-specific infection

One individual (/25: 4%), >46 year old male [128], had evidence of periosteal lesions on the lateral shafts of the tibiae. The condition affected 5.9% (1/17) of right and 5.6% (1/18) of left tibiae within the sample. This form of lesion reflects soft tissue inflammation that may result from both infectious and non-infectious forms of disease (trauma, scurvy, venous stasis, secondary hypertrophic osteoarthropathy and neoplastic disease) (Resnick 2002, 4884; Ortner 2003, 88).

4.6.3.2 Yersinia pestis

The burials were found in the area of a documented Black Death cemetery (Stow 1908). The *Yersinia pestis* pathogen was identified by Dr Hendrik Poinar of McMaster University in four individuals (/25: 16%) by aDNA analysis (Table 16; Table 17). Each of these individuals was exposed to, and may well have died from, one of the forms of plague (bubonic, pneumonic, septicaemic). As only 12 individuals were sampled and tested for the disease (/12: 33.3%) there was almost certainly a higher disease load in the population.

Context	Poinar ID	Phase	Sex	Age at death (years)
137	HP2275	3	Female	36–45
140	HP2276	3	Male	18–25

159	HP2273	2	Male	18–25
191	HP2271	1	?Male	26–35

Table 16 Individuals where Yersinia pestis was identified

Sample	Subsamples	# replicates	Libraries sequenced	Shotgun %yp (24+ bp assemblies)	BLAST results
CR04	CR04a	0 of 4			
	CR04c	1 of 4			
	CR04d	0 of 4	LC04d	0.00228%	2/519 reads Yp
CR06	CR04a	0 of 4			
	CR06c	1 of 4			
	CR06d	2 of 4	LC06d	0.00127%	1/319 reads Yp
CR08	CR08a	1 of 4			
	CR08c	0 of 4			
	CR08d	0 of 4	LC08d	0.00180%	2/371 reads Yp
CR09	CR09a				
	CR09c	1 of 4			
	CR09d	0 of 4	LC09d	0.00218%	4/454 reads Yp

*** "c" extracts were not used for shotgun sequencing because the phenol was not at the correct pH during extractions

For comparison, same information on Manching-Pichl sample

Sample	Subsamples	# replicates	Libraries sequenced	Shotgun %yp (24+ bp assemblies)	BLAST results
P11	P11a	1 of 4			
	P11b	3 of 4	LP11b	0.00544%	55/380 reads Yp
	P11c	4 of 4			

Table 17 SHOTGUN analysis results

4.6.4 Trauma

All traumatic lesions identified within the burial sample were bone fractures. The total crude prevalence of 28% (7/25) of individuals was slightly higher than that from St Mary Spital period 16 (1250–1400) (21.1%) and much higher than East Smithfield (male 14.8%, female 8.7%) (Table 18) (http://www.museumoflondon.org.uk/Collections-Research; Connell et al 2012, 89). Only adults were affected. Females had a higher rate of bone fracture when compared to males, though this was based on a small sample size. Injuries were spread throughout the adult age ranges (Table 19). All but one of the lesions was healed by the time of death.

	n	**Affected**	**%**
All	25	7	28.0
Subadults	2	0	-
Adults	23	7	30.4

Males	13	5	38.5
Females	3	2	66.7

Table 18 Fracture crude prevalence

Age (years)	n	Affected	%
18-25	6	1	16.7
26-35	3	2	66.7
36-45	5	2	40.0
≥46	3	2	66.7

Table 19 Fracture crude prevalence by age

Fracture location was predominantly restricted to the torso and upper limb (Table 20). However, two further fractures, affecting joint surfaces, were identified in the lower limb: an unhealed transverse fracture of the left patella of 26–35 year old male [137] possibly resulting from a stumble (Galloway 1999, 186), and a healed plateau fracture in the lateral condyle of the left tibia, often caused by tibial abduction (lateral movement of the tibia relative to the knee) (ibid 189) (Table 21).

	Adult			All individuals		
	n	Affected	%	n	Affected	%
Right parietal	16	1	6.3	18	1	5.6
Left rib	14	1	7.1	16	1	6.3
Right ulna	15	1	6.7	17	1	5.9
Left ulna	14	1	7.1	16	1	6.3
Right 1st metacarpal	10	1	10.0	11	1	9.1

Table 20 Fracture true prevalence

	Adult			All individuals		
	n	Affected	%	n	Affected	%
Left patella	12	1	8.3	13	1	7.7
Left tibia	12	1	8.3	13	1	7.7

Table 21 Joint surface fracture true prevalence

The only evidence of cranial trauma was found in 18–25 male [146] who had a small, well-healed blunt force injury to the right parietal.

A particularly severe example of a first right metacarpal fracture was found in 26–35 year old male [143], who had a healed comminuted extra-articular fracture of the first right metacarpal, with severe shortening and anterior and medial deviation, possibly reflecting a complex fracture with bone loss (Fig 12). As this type of injury normally requires direct force it may result from a severe blow to the hand (http://www.maitrise-orthop.com/viewPage_us.do?id=752 fig 21c). Severe deformity had occurred reducing the dexterity of this individual and quite likely his ability to work.

Fig 12 Healed first right metacarpal fracture in XTE12 [143] (temporary image)

Two ulna fractures were identified, both in ≥46 year old males ([128] and [153]) from the final phase of the cemetery (Fig 13). This equated to 6.9% (2/29) of adult ulnae and 8.3 (2/24) of male ulnae. At St Mary Spital, 2.3% (83/3576) of male ulnae were fractured (period 16 26/957: 2.7%) (Connell et al 2012, 97). In both cases, the fractures were isolated, non-displaced and affected the distal shafts. This type of fracture is often referred to as a 'parry fracture'.

Fig 13 Healed right ulna fracture in XTE12 [128] (temporary image)

There was one example of trauma in the first phase of the cemetery (1/11: 9.1%) and none in the second phase. Most was found in the third and final phase (6/12: 50.0%).

4.6.4.1 Dental trauma

Male adult [152] had a chipped mesial edge on the first right maxillary molar, possibly caused by indirect trauma to the skull or simply by biting down on a hard food particle.

4.6.5 Joint disease

4.6.5.1 Spinal joint disease

Fifteen individuals (15/25: 60%), one subadult and fourteen adults, had vertebral joint disease. Consistently high rates of osteophytes and Schmorl's nodes were encountered (Table 22). Osteoarthritis and the formation of osteophytes are a normal accompaniment of ageing and, in the absence of other abnormalities, are not considered pathological (Rogers and Waldron 1995, 25). More than 80% of males were affected by Schmorl's nodes, lesions resulting from intervertebral disc displacement and herniation. This suggests that the population represented by the sample were engaged in strenuous labour, perhaps from an early age, although lesions can also result from osteoporosis, skeletal metastases and Scheuermann's disease (Rogers and Waldron 1995, 27; Aufderheide and Rodríguez-Martín 1998, 97; Resnick 2002, 1430). Similar prevalence rates were observed in males from St Mary Spital period 16 (725/1192: 60.8%).

		Osteoarthritis		**Osteophytes**		**Intervertebral disc disease**		**Schmorl's nodes**	
	n	**Affected**	**%**	**Affected**	**%**	**Affected**	**%**	**Affected**	**%**
All	25	7	28.0	10	40.0	2	8.0	13	52.0
Subadult	2	0	-	0	-	0	-	1	50.0
Adult	23	7	30.4	10	43.5	2	8.7	12	52.2
Male	13	5	38.5	8	61.5	1	7.7	11	84.6
Female	3	2	66.7	2	66.7	1	33.3	1	33.3

Table 22 Spinal joint disease crude prevalence

There was a higher crude prevalence of individuals with Schmorl's nodes in phase 3 when compared to phase 1 (Table 23). However, this difference was not statistically significant.

Phase	n	Affected	%
1	11	4	36.4
2	2	2	100.0
3	12	8	66.7

Table 23 Schmorl's nodes crude prevalence by cemetery phase

Basic true prevalence rates of spinal joint disease are given below (Table 24).

		Osteoarthritis		**Osteophytes**		**Intervertebral disc disease**		**Schmorl's nodes**	
	n	**Affected**	**%**	**Affected**	**%**	**Affected**	**%**	**Affected**	**%**
All	403	18	4.5	74	18.4	5	1.2	86	21.3
Subadult	50	0	-	0	-	0	-	2	4.0
Adult	353	18	5.1	74	21.0	5	1.4	84	23.8
Male	294	12	4.1	46	15.6	1	0.3	83	28.2
Female	59	6	10.2	28	47.5	4	6.8	1	1.7

Table 24 Spinal joint disease true prevalence

4.6.5.1.1 DIFFUSE IDIOPATHIC SKELETAL HYPEROSTOSIS

Mature adult male [128] had large 'flowing candlewax' type vertebral osteophytes causing fusion of four contiguous vertebrae (ninth to twelfth thoracic) through ossification of the anterior longitudinal ligament. This, together with enthesopathic involvement of the ilia, femora and fibulae, was typical of DISH, a condition associated with advancing age and which has been linked to obesity and diabetes (Resnick 2002, 1478, 1496–7).

Fig 14 Osteophytes and fusion of ninth to 12th thoracic vertebrae of XTE12 [128] (temporary image)

4.6.5.2 Extra spinal joint disease

4.6.5.2.1 OSTEOARTHRITIS

Only those joint surfaces with eburnation were classified as having osteoarthritis (Rogers and Waldron 1995). Two 36–45 year old males were affected, both in the right acromioclavicular joints of the shoulder (Table 25) (Table 26).

	n	Affected	%
All	25	2	8.0
Subadults	2	0	-
Adults	23	2	8.7
Males	13	2	15.4
Females	3	0	0.0

Table 25 Crude prevalence of extra spinal osteoarthritis

		Male			All adults		
Joint		**n**	**Affected**	**%**	**n**	**Affected**	**%**
Acromioclavicular	Right	11	2	18.2	12	2	16.7
	Left	11	0	-	12	0	-
	Total	22	2	9.1	24	2	8.3

Table 26 True prevalence of extra spinal osteoarthritis

4.6.5.2.2 ROTATOR CUFF

Two individuals, both aged 36–45 years, had lesions typical of rotator cuff injuries: male [152] (bilateral) and female [137] (left side only).

4.6.5.2.3 JOINT ANKYLOSIS

Adult male [152], aged 36–45 years, had anterior fusion of the left sacroiliac joint caused by ossification of the anterior sacroiliac ligament. The right joint was present but unaffected. This condition is associated with increasing age (http://www.ajronline.org/doi/pdf/10.2214/ajr.128.2.189).

4.6.6 Metabolic disease

4.6.6.1 Rickets

Vitamin D deficiency in infancy and childhood, known as rickets, can lead to inadequate levels of bone mineralisation. Rickets affects both the healthy maintenance of bone and its formation. It is most commonly caused by a lack of exposure to ultraviolet light from the sun, although it can also arise from digestive disorders affecting vitamin D metabolism (Ortner 2003, 393; Mays et al 2006, 362). Such deficiency can cause weight-bearing and loaded bones to bend, sometimes to extreme extents, whilst other areas of the skeleton can develop porosity. Crowded and polluted urban environments, together with social practices and overprotective clothing can prevent sufficient exposure to ultraviolet light (ibid, 393–4). Although rickets only occurs in childhood, the residual effects can sometimes be observed in the adult skeleton, particularly where an individual was severely affected, but survived.

Four adults had evidence of residual rickets: 17.4% of adults and 16.0% of the total sample. Prevalence rates were far higher than that observed at East Smithfield (2/636: 0.3%) and St Mary Spital (8/5387: 0.1%) (http://www.museumoflondon.org.uk/Collections-Research; Connell et al 2012, 119).

4.6.7 Circulatory disease

4.6.7.1 Osteochondritis dissecans

Osteochondritis dissecans involves the fragmentation of cartilage and subchondral bone within a joint, probably most often as a result of trauma in adolescence, although it has also been described as idiopathic (Aufderheide and Rodríguez-Martín 1998, 81–2; Ortner 2003, 351). There were two examples of this condition (8.0%) in the third phase of the cemetery at Charterhouse Square, both involving fragmentation of the femoropatellar joint of the knee.

4.6.8 Other pathological conditions

4.6.8.1 Cribra orbitalia

Cribra orbitalia, or porotic lesions in the orbits of the cranium, has been linked to megaloblastic or iron-deficiency anaemia resulting from blood loss, malnutrition and gastrointestinal disease (Roberts and Cox 2003, 234; Walker et al 2009). It is believed to have a similar aetiology to porotic hyperostosis of the cranial vault, although the relationship is not fully understood (Aufderheide and Rodríguez-Martín 1998, 350). Of 50 possible orbits from 25 individuals, 27 (54%) were sufficiently preserved for examination (Table 27). Of these, 10 (/27: 37.0) had porotic lesions of low severity (Stuart-Macadam 1991, 109).

			Grade		
	Not present	**n**	**0**	**1**	**2**
Left	12	13	8	4	1
Right	11	14	9	4	1
Total	**23**	**27**	**17**	**8**	**2**

Table 27 Cribra orbitalia summary and grading (by orbit)

The crude prevalence rate of individuals, with one or more orbits observable, with cribra orbitalia was 20% (5/25) (Table 28). Sixty per cent of individuals (3/5) from phase 1 and 25% (2/8) from phase 3 were affected. Three individuals aged over 35 years of age (/6: 50%) had cribra orbitalia compared to two (/9: 22.2%) below this age, both of whom were subadults.

	n	**Affected**	**%**
All	25	5	20.0
Subadults	2	2	100.0
Adults	23	3	13.0
Males	13	2	15.4
Females	3	1	33.3

Table 28 Cribra orbitalia crude prevalence (1 or more orbits affected)

Cribra orbitalia was also calculated by orbit (Table 29). The prevalence rates were higher than those at East Smithfield (Adult: left 10.2%, right 9.4%. Subadult: left 10.2%, right 10.6%) and at period 16 St Mary Spital (http://www.museumoflondon.org.uk/Collections-Research; Connell et al 2012, 122). No - deleted

	Total			**Adult**			**Subadult**		
	n	**Affected**	**%**	**n**	**Affected**	**%**	**n**	**Affected**	**%**
Left	13	5	38.5	11	3	27.3	2	2	100.0
Right	14	5	35.7	12	3	25.0	2	2	100.0

Table 29 Cribra orbitalia by orbit

4.6.8.2 Porotic hyperostosis

Three males, one from phase 1 and two from phase 3 of the cemetery, had healed cranial porotic lesions typical of porotic hyperostosis. All were aged 35 years or younger at death.

5 Discussion and conclusions

The Black Death reached England in the summer or autumn of 1348, perhaps as early as June or as late as October, and had spread to London by November (Sloane 2011, 29, 33–4). By its decline in 1350, it had killed between one third and one half of the population. The Black Death has traditionally been associated with plague (*Yersinia pestis*), a specific zoonosis in rodents and their fleas (Aufderheide and Rodríguez-Martín 1998, 195). Of the three manifestations of the disease, bubonic plague is the most common. It is spread to humans by the bite of infected fleas and attacks the lymphatic system resulting in fever, headache, chills and painful swollen lymph nodes called buboes. These buboes are characteristic of the disease and usually appear at the lymph nodes sited closest to the infected bite, either at the neck, under the arm or in the groin. As the disease progresses the swollen nodes darken in colour from red to black giving the Black Death its name. The disease resolves within days with a 60 to 70 per cent mortality rate (Roberts and Cox 2003, 266). A second form, septicaemic plague, can appear independently or can develop from the bubonic form. It affects the blood stream and kills through diffuse haemorrhage. It can cause necrosis in the extremities, leading to tissue death in the nose, fingers and toes. The third form, pneumonic plague, affects the respiratory system producing bloody sputum and is invariably fatal in the absence of antibiotics. Pneumonic plague can be spread directly from human to human through droplet infection, or can develop secondary to the bubonic or septicaemic forms (Aufderheide and Rodríguez-Martín 1998, 196; Roberts and Cox 2003, 266). The articulated skeletal assemblage from two rows of inhumations at Charterhouse Square is small but significant in that the burial ground from which it originates is within the area of a documented Black Death cemetery (Stow 1908). The burial ground was reportedly for the use of 'poor strangers (*peregrinorum*) and others' (Sloane 2011, 46).

Another Black Death burial ground in London, at East Smithfield, contained a large number of single inhumations arranged in rows (Grainger et al 2008, 11). Although mass burial trenches and a pit were dug there, they may only have been required during mortality peaks and even then the trench was not intensively filled. Both East and West Smithfield cemeteries were opened in late 1348 or early 1349 (Grainger et al 2008, 29). Perhaps this planned and organised approach to the arrival of the great mortality shows that something had been learned from the emergency use of existing burial grounds such as St Mary Spital a century earlier (Connell et al 2012, 217–8).

Recent technological advances in genetic science have resulted in a surge of interest in the study of ancient DNA. Improved recovery and sequencing techniques were employed on samples from East Smithfield, from where the first draft genome of 14th century *Yersinia pestis* was obtained (Bos et al 2011).

Following aDNA analysis, the presence of the pathogen *Yersinia pestis* has now been established in the skeletal remains of four of the 12 sampled individuals at Charterhouse Square. The four affected individuals were spread throughout the three phases of burial. Therefore, each burial phase must have been contemporary with one of the many outbreaks of the disease in London. Did all three burial phases result from the same outbreak or from two or three different episodes, and can we identify them? As Spital Croft was first opened as a burial ground specifically for the 1348–9 Black Death it is reasonable to accept that the earliest phase of burial containing 11 articulated individuals belonged to this episode, provided that the part of the ground lying in the south-west corner of Charterhouse Square was in use at that time. There was some disarticulated bone in the grave fills of some of the earliest burials, although this comes from the limits of the excavation and may be intrusive. The smaller second phase of

burial, containing just two individuals, may have been associated with the same outbreak. The alignment was the same as the earlier phase and did not disturb any of the previous burials, suggesting their position, depth and orientation were still obvious above ground, either through remaining mounds of earth or grave markers. At the same time, the results of the radiocarbon dating do not dismiss the possibility that one or both of the first two phases of burial were later in the second half of the 14th century. Therefore, they could be contemporary with a later outbreak of plague. In this there may be a precedent at London's other Black Death burial ground. Sloane argues that East Smithfield was used to bury victims of the Pestis Secunda (1361–2) (2011, 136–40). This epidemic was not as devastating as the first outbreak but was a cause of significant mortality to the extent that we might expect to see it reflected in the archaeological record.

The shift in burial alignment at Charterhouse Square (from south-west/north-east to west/east) represents a change in funerary practice in the third and final phase, albeit a subtle one. Those responsible for siting and digging the graves may have been following a new alignment, perhaps one based on the orientation of a new building, path or fence. It is possible that the strict west-east alignment mirrored that of the walls of a new construction such as a cemetery chapel. Alternatively, it is quite plausible that those responsible for the siting and digging of graves were replaced by new workers who were either not aware or were unconcerned with the exact alignment of previous graves. Following the results of radiocarbon dating, it can now be confirmed that the 12 burials from this phase probably date to after 1400 and belong to a period of activity distinct from the first two phases. This is crucial evidence, as it demonstrates re-use of the cemetery during later episodes of plague.

It also supports the other archaeological evidence such as the lack of skeletal articulation in the re-deposited remains from phase 2, which suggested that sufficient time had elapsed between phase 2 and 3 for the soft tissues, including the ligaments that hold bones together, to decompose. The factors governing the stages and timing of soft tissue decomposition are many and varied, but the bones of human bodies buried in the ground may remain attached and in articulation for a number of years (Mann et al 1990). At St Mary Spital articulated limbs from disturbed mass burial pits were disturbed after perhaps less than 10 years in the ground and re-deposited in a later phase of pits (Connell et al 2012, 218). The fact that the remains were articulated hinted that the two phases of mass burial were not separated by a long period of time. Of course it is impossible to know how long after death a person was buried, particularly in times of extreme stress, and the stage of decomposition reached prior to interment is a further variable.

In summary, it is clear that there was temporal separation between the second and third phases of burial at Charterhouse Square, but the length of time is difficult to define. The radiocarbon dates have demonstrated that there was continuity of use with perhaps several decades separating the final two phases. They further show, in combination with the aDNA results that individuals exposed to plague continued to be buried at Charterhouse after the monastic foundation in 1371. Many of those exposed to the plague would have died from it so it appears that the burial ground continued to be used as a plague cemetery.

The study of the prevalence and distribution of pathological lesions within the skeletal assemblage has produced some interesting results, albeit based on a small sample size. Most bone fractures were found within the third and final phase of the cemetery. As this phase of burials belonged to a later outbreak of plague, it is tempting to speculate that the injuries were sustained during an earlier epidemic, reflecting a rise in lawlessness and injury risk at a time of

heightened social stress. There were of course other causes of discontent in this period, such as the Peasants' Revolt of 1381. The high prevalence of isolated non-displaced ulna fractures, although based on a low sample size, points to a phenomenon previously identified in medieval burials from London. The mechanism of such fractures in the past is uncertain. In modern clinical medicine, they can result either from falls where the arm strikes the edge of a surface, from repetitive strain perhaps related to occupational activity or from parrying a blow from an assailant (Lovell 1997, 165; Judd 2004, 46). We don't know whether these injuries were the result of accidental injury or interpersonal violence, but recent work has suggested the ulna was the most commonly fractured long bone in medieval London (Connell et al 2012, 95, 182–3). Other examples of lesions with a traumatic aetiology from phase 3 included the severe first metacarpal fracture in 26–35 year old male [143], and two cases of osteochondritis dissecans.

Prevalence rates of Schmorl's nodes indicate high levels of strenuous activity or load bearing in the burial sample, reflecting results from other medieval cemeteries in London. This together with the relatively high prevalence of rickets could be taken to support documentary evidence that the cemetery was for the burial of poor strangers. However, it is based on a small sample size, as is the metric data that suggests males buried at Charterhouse Square attained greater living stature when compared to other contemporary burial samples. The individual stature measurements lay within the range found at other medieval cemetery sites in London.

Strontium and oxygen stable isotope analysis carried out at Durham University and University of Bradford on tooth enamel samples from ten individuals identified six who were likely to have been indigenous to London ([134], [143], [146], [152], [185] and [188]). The other four individuals grew up outside London, [159] most likely in eastern England, [140] and [194] most likely in central or eastern England and [182] most likely in northern England or Scotland (Montgomery et al 2014). Migration to towns from rural communities was a feature of the medieval period so this is not a surprising result (Keene 1989, 104; Dyer 1998, 109–87; Goldberg 1997, 12; Sheppard 1998, 115; Singman 1999, 26, 67; Dyer 2002, 187). The stable isotope analysis shows that migrants were moving to London not only from the southern and eastern areas of England, but from further afield. The four non-indigenous individuals were spread through all three phases of burial.

Interestingly, the carbon and nitrogen stable isotope results indicated that all but one of the individuals with evidence of nutritional or health stress were of local origin (Montgomery et al 2014). The opportunities of the medieval town attracted people from outside but there may have been consequences for standards of living, particularly in those most sensitive to ill health, the children.

The carbon isotope results reveal a diet ranging from one based predominantly on terrestrial foods to one of mixed terrestrial and marine foods. The nitrogen isotopes produce a range from predominantly plant based diets to those containing both plant and animal protein (meat or milk). Some of the 'meat' protein may be formed by a combination of terrestrial and marine based foods (Montgomery et al 2014).

By combining the osteological and stable isotope analysis it is possible to build up a remarkably detailed picture of an individual's life. Context [140], a male individual, may have been born in central or eastern England, and appears to have been breastfed as an infant. Sometime between approximately one and two years of age he suffered some form of stress, perhaps illness or malnutrition, reflected in hypoplastic lines in the teeth. At the age of about five years, he moved to London where his diet, which may have been plant-based, stabilised. During later childhood, he suffered from Schmorl's nodes in the vertebral column reflecting

strenuous activity, together with a tooth abscess. He would have been affected by chronic pain from severe dental cavities in his molar teeth, possibly through much of his childhood, but certainly in later adolescence. Having been exposed to *Yersinia pestis*, he died sometime in the first half of the 15th century between the ages of 18 and 25 years, quite possibly from plague. He was then buried at Charterhouse.

Context [134], a male individual raised in London was born with a congenital disorder at the junction of his lumbar and sacral vertebral columns, although it is not clear to what extent, if any, this affected his everyday life. As with context [140], he suffered some form of stress between approximately one and two years of age. He also had Schmorl's nodes and was in fact affected more severely than [140]. Osteochondritis dissecans in his right femur may have resulted from activity-related trauma to the knee during adolescence. Between the ages of 11 and 20 he had a significant change in protein consumption, possibly from meat to plant based foods. He died between the ages of 18 and 25 and was buried in the plague cemetery at Charterhouse sometime in the first half of the 15th century. We do not know if he was either exposed to, or died from, plague.

Identifying fluctuations in protein consumption cannot tell us why they took place. In the third phase of burials at Charterhouse it is tempting to think that changes to plant based diets may indicate novices at the priory taking up the Carthusian way of life with its strict vegetarian diet. However, such shifts in diet could affect both sexes. Probable female [194], who was raised in central or eastern England, may have changed from a meat to plant-based diet around the time she came to London after the age of 16. This may have pre-dated the foundation of the Charterhouse. She died during an outbreak of plague, possibly soon after the disease arrived in London in 1348.

Male [159] was brought up somewhere on the chalkland of eastern England. He had some episode of disease or malnutrition between two and four years of age. At some stage he suffered severe Schmorl's nodes, reflecting strenuous activity. After the age of 16 years he moved to London where, at around the age of 21, the marine proportion of the protein in his diet increased. After being exposed to plague, he died between the ages of 18 and 25 years, perhaps during the initial outbreak of the disease in London, or a later epidemic such as the Pestis Secunda.

Overall, the results of the stable isotope analysis demonstrate variation in the residential and dietary histories of the ten individuals from Charterhouse, a remarkable insight into the lives of medieval Londoners (Montgomery et al 2014). Summaries of the results for each context are listed in the appendix (Table 30).

Further work will look at how the *Yersinia pestis* pathogen from Charterhouse Square compares to that from East Smithfield. It will also study the genome in more detail, in order to understand the genetic basis behind epidemiological variations between ancient and modern plague. This would be part of larger projects using high throughput molecular analysis to examine disease ecology and its possible contribution to mortality during plague outbreaks, as well as human health and genetic variation before and after the Black Death.

6 Bibliography

Aufderheide, A C, and Rodríguez-Martín, C, 1998 *The Cambridge encyclopaedia of human paleopathology*, Cambridge

Barber, B, and Thomas, C, 2002 *The London Charterhouse*, MoLAS Monogr 10, London

Barnes, E, 1994 Developmental defects of the axial skeleton in palaeopathology, Colorado

Blackmore, L, 2014 The medieval pottery from Crossrail works at Charterhouse (XTE12), unpublished report, MOLA

Bos, KI, Schuenemann, VJ, Golding, GB, Burbano, HA, Waglechner, N, Coombes, BK, McPhee, JB, DeWitte, SN, Myer, M, Schmedes, S, Wood, J, Earn, DJD, Herring, DA, Bauer, P, Poinar, HN, and Krause J, 2011 A draft genome of Yersinia pestis from victims of the Black Death, *Nature* 478, 506–10

Brooks, S T and Suchey, J M 1990 Skeletal Age Determination Based on the Os Pubis: a comparison of the Ascadi-Nemeskeri and Suchey-Brooks methods, *Human Evolution* 5, 227–38

Brothwell, D, 1981 *Digging Up Bones*, London

Connell, B, and Rauxloh, P, 2003 *A rapid method for recording human skeletal data,* Second edition revised 2007 Powers, N (ed)

Connell, B, Gray Jones, A, Redfern, R, and Walker, D, 2012 *Spitalfields: a bioarchaeological study of health and disease from medieval London: a*rchaeological excavations at Spitalfields Market 1991–2007, volume 3. MOLA monograph

Dyer, C, 1998 *Standards of living in the later Middle Ages: social change in England* c *1200–1500*, rev edn, Cambridge

Dyer, C, 2002 *Making a living in the Middle Age*s, London

Galloway, A (ed), 1999 *Broken bones: anthropological analysis of blunt force trauma,* Springfield, IL.

Goldberg, P J P, 1997 Marriage, migration, and servanthood: the York Cause paper evidence, in *Women in medieval English society* (ed P J P Goldberg), 1–15, Oxford

Grainger, I, Hawkins, D, Cowal, L, and Mikulski, R, 2008 *The Black Death cemetery, East Smithfield, London*, MoLAS Monogr Ser 43, London

Gustafson, G, and Koch, G, 1974 Age estimation up to 16 years of age based on dental development, *Odontologisk Revy* 25, 297–306

Hillson, S, 1996 *Dental Anthropology*, Cambridge

Iscan, M Y, Loth, S R, and Wright, R K, 1984 Age estimation from the rib by phase analysis: white males, *Journal of Forensic Science* 29, 1094-1104

Iscan, M Y, Loth, S R, and Wright, R K, 1985 Age estimation from the rib by phase analysis: white females, *Journal of Forensic Science* 30, 853-863

Judd, M, 2004 Trauma in the city of Kerma: ancient versus modern injury patterns, *Int J Osteoarchaeol* 14, 34–51

Keene, D J, 1989 Medieval London and its region, *London J* 14(2), 99–111

Lovejoy, C, Meindl, R, Pryzbeck, T and Mensforth, R, 1985 Chronological metamorphosis of the auricular surface of the ilium: a new method for the determination of age at death, *American Journal of Physical Anthropology* 68, 47–56

Lovell, N C, 1997 Trauma analysis in paleopathology, *Yearbook Phys Anthropol* 40, 139–70

Mann, R W, Bass, W M, and Meadows, L, 1990 Time since death and decomposition of the human body: variables and observations in case and experimental field studies, *Journal of Forensic Sciences* 35, 103–11

Maresh, M M, 1970 Measurements from roentgenograms, in *Human Growth and Development (ed.* R W Mc Cammon), Springfield, 157–200

Mays, S, Brickley, M, and Ives, R, 2006 Skeletal manifestations of rickets in infants and young children in a historic population from England, *Amer J Phys Anthropol* 129, 362-74

MOLA for Crossrail 2012a C257 Archaeology Central Farringdon Eastern Ticket Hall Fieldwork Report Archaeological Targeted Watching Brief RBS Trial Trench , 23–28 Charterhouse Square, Farringdon (XSF10) Doc. No.: C257-MLA-X-RGN-CRG02-50073 Revision 2.0, 08.03.12

MOLA for Crossrail 2012b C257 Archaeology Central Fieldwork Report Archaeological Targeted and General Watching Brief at Farringdon Eastern Ticket Hall Utilities Diversions (XSF10) Doc. No.: C257-MLA-X-RGN-CRG02-50117 Revision 2.0, 06.07.12

Montgomery, J, Beaumont, J, Towers, J, and Nowell, G, 2014 Isotope analysis of the Charterhouse skeletons undertaken on behalf of Crossrail and MOLA, unpublished final report

Moorrees, C F A, Fanning, E A. and Hunt, E E Jr. 1963a Formation and resorption of three deciduous teeth in children, *American Journal of Physical Anthropology* 21, 205–13

Moorrees, C F A, Fanning, E A and Hunt, E E Jr. 1963b Age variation of formation stages for ten permanent teeth, *Journal of Dental Research* 42(6), 1490–1502

Ortner, D J, 2003 *Identification of pathological conditions in human skeletal remains,* London

Pfizenmaier, S, 2013 Crossrail Farringdon Eastern Ticket Hall. Charterhouse Square Grout Shaft, London EC1, unpublished post-excavation assessment and updated project design, MOLA

Powers, N (ed), 2008 *Human Osteology Method Statement*. Museum of London on-line publication

Resnick, D, 2002 *Diagnosis of bone and joint disorders*, Philadelphia

Roberts, C, and Connell, B 2004 Palaeopathology, in *Guidelines to the Standards for Recording Human Remains* (eds M Brickley and J McKinley), IFA paper no. 7

Roberts, C A, and Cox, M, 2003 *Health and disease in Britain*, Stroud

Rogers, J, and Waldron, T, 1995 *A field guide to joint disease in archaeology,* Chichester

Ruddy, M, 2014 Radiocarbon dating and Baysian modelling for Charterhouse (Crossrail) XTE12, unpublished report, MOLA

Scheuer, L, and Black, S, 2000 *Developmental Juvenile Osteology*, London

Schuenemann, VJ, Bos, K, DeWitte, S, Schmedes, S, Jamieson, J, Mittnik, A, Forrest, S, Coombes, BK, Wood, JW, Earn, DJD, White, W, Krause, J, and Poinar, HN, 2011 Targeted enrichment of

ancient pathogens yielding the pPCP1 plasmid of Yersinia pestis from victims of the Black Death, *Proceedings of the National Academy of Sciences* 108, E746-E752

Sheppard, F, 1998 *London: a history*, Oxford

Singman, J L, 1999 *Daily life in medieval Europe*, London

Sloane, B, 2011 The Black Death in London, Stroud

Stow, J, 1908, *A Survey of London Reprinted from the text of 1603* Vol 1

Stuart-Macadam, P L, 1991 Anaemia in Roman Britain; Poundbury Camp, in *Health in past societies. Biocultural interpretations of human skeletal remains in archaeological contexts* (eds H Bush and M Zvelebil), BAR Brit Ser 567, 101-113, Oxford

Trotter, M, 1970 Estimation of stature from intact long limb bones, in *Personal Identification in Mass Disasters* (ed. T D Stewart), Washington

Tyrell, A, 2000 Skeletal non-metric traits and the assessment of inter- and intra-population diversity: past problems and future potential, in Cox, M and Mays, S (eds) *Human Osteology in Archaeology and Forensic Science,* London, 289–3060

Walker, P L, Bathurst R R, Richman, R, Gjerdrum, T, and Andrushko, V A, 2009 The causes of porotic hyperostosis and cribra orbitalia: A reappraisal of the iron-deficiency-anemia hypothesis, *American Journal of Physical Anthropology* 139, 109–25

http://www.ajronline.org/doi/pdf/10.2214/ajr.128.2.189

http://www.maitrise-orthop.com/viewPage_us.do?id=752

http://www.museumoflondon.org.uk/Collections-Research

7 Appendix

7.1.1 Articulated bone

Context	Preservation	Sex	Age	Pathology summary	Origin	Health stress and diet	Comments
128	Good	Male	≥46 years	R.ulna fracture, residual rickets, spondylolysis, DISH, tibiae periostitis, bifid rib, Schmorl's nodes			Phase 3. Legs truncated by machine
131	Moderate	Female	≥46 years	Left patella osteochondritis dissecans, Schmorl's nodes			Phase 3
134	Good	Male	18–25 years	Right femur osteochondritis dissecans, vertebral bifurcation, hypoplasia and border shift, enamel hypoplasia, periodontal disease, Schmorl's nodes	Local	Poss. change from meat to plant diet 11–20 years	Phase 3
137	Moderate	Female	36–45 years	*Yersinia pestis*, rib fracture, left patella unhealed fracture, rotator cuff, cribra orbitalia, dental caries, periodontal disease, periapical lesion, Schmorl's nodes			Phase 3. Truncated by limit of excavation
140	Good	Male	18–25 years	*Yersinia pestis*, severe dental caries, enamel hypoplasia, periodontal disease, periapical lesion, Schmorl's nodes	Non-local. Moved to London	Breast fed in infancy coupled with nutritional/	Phase 3. Legs truncated by machine

					after age of 5	health stress. Diet stabilises after age of 5. Plant based diet?	
143	Good	Male	26–35 years	Severe first right metacarpal fracture, porotic hyperostosis, dental caries, enamel hypoplasia, periodontal disease, Schmorl's nodes	Local	Dietary variation between 6.5–11 years. Nutritional/ health stress 12–15 years	Phase 3. Legs truncated by machine
146	Good	Probable male	18–25 years	Residual rickets, porotic hyperostosis, blunt force trauma, spina bifida occulta, dental caries, periodontal disease, Schmorl's nodes	Local	Nutritional/ health stress ?–10 and 17–23 years? Probable marine protein consumer	Phase 3
149	Good	Probable male	36–45 years	None			Phase 3. Truncated by limit of excavation
152	Moderate	Male	36–45 years	Sacroilitis, rotator cuff, dental trauma, caries, enamel hypoplasia, periodontal	Local		Phase 3. Double burial with

				disease, periapical lesion, Schmorl's nodes			153
153	Moderate	Probable male	≥46 years	Left ulna fracture, cribra orbitalia, periodontal disease, Schmorl's nodes			Phase 3. Double burial with 152. Cranium from fill 151.
156	Good	Probable male	36–45 years	Right acromioclavicular osteoarthritis, periodontal disease, Schmorl's nodes			Phase 2
159	Moderate	Male	18–25 years	*Yersinia pestis*, enamel hypoplasia, periodontal disease, Schmorl's nodes	Non-local. Moved to London from a chalk region after age of 16	Increase in marine protein *c*21 years	Phase 2. Legs and feet recovered from fill 142
163	Good	Undetermined	18–25 years	Residual rickets			Phase 1. Truncated by limit of excavation
166	Moderate	Undetermined	Adult	None			Phase 3. Truncated by limit of excavation
167	Good	Undetermined	Adult	None			Phase 3.

							Truncated by limit of excavation
170	Good	Undetermined	Adult	None			Phase 1. Truncated by limit of excavation. Right talus and navicular recovered from fill 169.
173	Moderate	Undetermined	Adult	None			Phase 1. Truncated by limit of excavation
176	Good	Undetermined	Adult	None			Phase 1. Truncated by limit of excavation
179	Good	Undetermined	Adult	None			Phase 1. Truncated by limit of excavation
182	Good	Probable male	36–45 years	Cribra orbitalia, dental caries, periodontal disease, Schmorl's nodes	Non-local. Moved to London after age		Phase 1

					of 8		
185	Good	Subadult	12–17 years	Scoliosis, cribra orbitalia, dental caries, periodontal disease, Schmorl's nodes	Local	Possible nutritional / health stress 2.5–5 years	Phase 1. *c* 17 years, coffin base/board
188	Good	Male	26–35 years	Left tibia plateau fracture, periodontal disease, Schmorl's nodes	Local	Significant dietary changes in childhood. Nutritional/ health stress 4–8 years	Phase 1
191	Good	Probable male	26–35 years	*Yersinia pestis*, residual rickets, porotic hyperostosis, dental caries, periodontal disease, Schmorl's nodes			Phase 1
194	Good	Probable female	18–25 years	Periodontal disease	Non-local. Moved to London after age of 16	Change from meat to plant based diet at about age of 16	Phase 1. Truncated by limit of excavation
197	Moderate	Subadult	6–11 years	Cribra orbitalia, dental caries			Phase 1. *c* 8 years. Truncated by limit of excavation

Table 30 XTE12 Summary of articulated bone

7.1.2 Disarticulated bone

Context	Body area	Elements present	Age	Sex	Pathology	MNI	Comments
128	Upper limb	Left scapula	Adult	Undetermined	None	1	Intrusive bone
136	Upper limb	Right humerus	Adult	Undetermined	None	1	From grave fill of sk 137
153	Upper limb	Right humerus	Adult	Undetermined	None	1	Intrusive bone
161	Skull	Right frontal	Adult	Undetermined	None	1	From levelling over first phase of burials
		Supraoccipital	Adult	Undetermined	None	1	From levelling over first phase of burials
	Torso	Sternum	Adult	Undetermined	None	1	From levelling over first phase of burials
		Right rib	Adult	Undetermined	None	1	From levelling over first phase of burials
	Upper limb	Left humerus	Adult	Undetermined	None	1	From levelling over first phase of burials
		Right radius	Adult	Undetermined	None	1	From levelling over first phase of burials
		Left radius	Adult	Undetermined	None	1	From levelling over first phase of burials
		Left ulna	Adult	Undetermined	None	1	From levelling over first phase of burials
		2 x unsided middle phalanges	Adult	Undetermined	None	1	From levelling over first phase of burials
		Right scapula	Subadult	1-5 years	None	1	From levelling over first phase of burials
	Lower limb	Right pubis	Adult	Undetermined	None	1	From levelling over first phase of burials
		Left pubis	Adult	Undetermined	None	1	From levelling over first phase of burials

		Right femur	Adult	Undetermined	None	1	From levelling over first phase of burials
		Left third metatarsals x 2	Adult	Undetermined	None	1	From levelling over first phase of burials
		Fourth left metatarsal	Adult	Undetermined	None	1	From levelling over first phase of burials
		Unsided proximal phalanx	Adult	Undetermined	None	1	From levelling over first phase of burials
166	Upper limb	Right scapula	Adult	Undetermined	None	1	Intrusive bone
		Right humerus	Adult	Undetermined	None	1	Intrusive bone
		Right radius	Adult	Undetermined	None	1	Intrusive bone
		Right ulna	Adult	Undetermined	None	1	Intrusive bone
176	Lower limb	Right navicular	Adult	Undetermined	None	1	Intrusive bone
		Right cuboid	Adult	Undetermined	None	1	Intrusive bone
		Right lateral cuneiform	Adult	Undetermined	None	1	Intrusive bone
		Left navicular	Adult	Undetermined	None	1	Intrusive bone
		Right metatarsals 1-5	Adult	Undetermined	None	1	Intrusive bone
		Left metatarsals 1-4	Adult	Undetermined	None	1	Intrusive bone
		Right proximal phalanx	Adult	Undetermined	None	1	Intrusive bone
		2 unsided proximal phalanges	Adult	Undetermined	None	1	Intrusive bone
178	Lower limb	Unsided proximal phalanx	Adult	Undetermined	None	1	From grave fill of sk 179
					Total MIN	**4**	

Table 31 XTE12 summary of disarticulated bone

Context	Body area	Elements present	Age	Sex	Pathology	MNI	Comments
66	Lower limb	Right femur	Adult	Undetermined	None	1	Missing proximal end, PM damage
	Upper limb	Right humerus	Subadult	-	None	1	Unfused proximal epiphyses, PM damage
		Left humerus	Adult	Undetermined	None	1	Missing proximal end, PM damage
		Unsided humeral midshaft	Adult	Undetermined	None	1	PM damage
		Right scapula	Adult	Undetermined	None	1	PM damage to blade, missing coracoid process
		Left ulna	Adult	Undetermined	None	1	Missing distal end
		Left radius	Adult	Undetermined	None	1	Missing distal end
		Left radius	Adult	Undetermined	None	1	missing proximal and distal end
	Thorax	First thoracic vertebrae	Adult	Undetermined	None	1	None
		Right rib	Adult	Undetermined	None	1	None
		Left ribs x 4	Adult	Undetermined	None	1	None
	Skull	Frontals, parietals, occipital	Adult	Female	None	1	Metopic suture, wormian bones
		Frontals, parietals, occipital, temporals, maxilla	Adult	Female	AMTL	1	Pm damage to L. parietal, FE stains
		Frontal, parietals, supra occipital	Adult	Probable female	None	1	Fragmented, metopic suture
		R. maxilla	Adult	Undetermined	Calculus	1	None
					Total MNI	**3**	

Table 32 XFS10 summary of disarticulated bone from Eastern Ticket Hall Utilities Diversions

Context	Body area	Elements present	Age	Sex	Pathology	MNI	Comments
71	Lower limb	Right femur	Adult	Undetermined	None	1	Post mortem breaks to proximal shaft, iron stains
		Right femur	Adult	Undetermined	None	1	Missing proximal and distal ends
		Left tibia	Adult	Undetermined	None	1	Missing distal end
					Total MNI	**2**	

Table 33 XFS10 summary of disarticulated bone from Eastern Ticket Hall RBS Trial Trench